First-Principles Investigation of the Early 3d Transition Metal Diatomic Chlorides and Their Ions, $ScCl^{0,\pm}$, $TiCl^{0,\pm}$, $VCl^{0,\pm}$, and $CrCl^{0,\pm}$

Stavros Kardahakis and Aristides Mavridis*

Laboratory of Physical Chemistry, Department of Chemistry, National and Kapodistrian University of Athens, P.O. Box 64 004, 15710 Zografou, Athens, Greece

Received: February 10, 2009; Revised Manuscript Received: March 26, 2009

The titled molecular species have been studied by ab initio multireference and coupled-cluster methods in conjunction with large correlation consistent basis sets. A total of 71 MCl, 13 MCl^+, and 9 MCl^- states, M = Sc, Ti, V, Cr, have been examined. We report total energies, dissocation energies, spectroscopic parameters, and full potential energy curves. Most of our results are presented for the first time in the literature, whereas the general agreement with available experimental data can be considered as quite good.

1. Introduction

The difficulties of obtaining accurate all-electron ab initio results for the ground and excited states of open-shell systems are well-known.[1] It is also known that these problems are accentuated in the case of open-shell molecules containing 3d transition metal atoms due to their special characteristics, i.e., high density of low-lying states and high space-spin angular momenta.[2]

We have recently completed the investigation of the electronic structure and bonding of the diatomic neutral fluorides MF, M = Sc−Cu,[3,4] as well as of the corresponding singly charged monofluorides $ScF^{\pm1}$, $TiF^{\pm1}$, $VF^{\pm1}$, $CrF^{\pm1}$, and $MnF^{\pm1}$,[5] through all-electron multireference variational and coupled-cluster calculations. The purpose of exploring the diatomic 3d transition metal halogenides, MX, has been discussed in refs 3 and 5 and will not be repeated here; see also ref 2.

Currently, we report high-level ab initio calculations for the ground and excited states of the neutral diatomics ScCl, TiCl, VCl, and CrCl. In particular, we report for the first time 21 (ScCl), 8 (TiCl), 15 (VCl), and 27 (CrCl) full potential energy curves (PEC) of the lowest of the MCl states. In addition, three, three, two, and one states and their PECs have been calculated for the anions $ScCl^-$, $TiCl^-$, VCl^-, and $CrCl^-$, respectively; for the corresponding cations, MCl^+, we have explored their ground and certain excited states around equilibrium. It should be stated at this point that despite the general interest on the MCl molecules, as testified by the large number of experimental works (vide infra), ab initio studies are indeed limited. For the anions in particular, there is a complete paucity of either experimental or theoretical results.

Similarly to our previous works,[3−5] in addition to PECs we report static molecular properties, namely, bond distances (r_e), dissociation energies (D_e), common spectroscopic parameters (ω_e, $\omega_e x_e$, α_e, $\bar{D}_e$), dipole moments (μ_e), and energy separations (T_e).

The paper is structured as follows: in section 2 we describe methodological details, in section 3 we discuss relevant results on the neutral atoms and their cations, sections 4 through 7 refer to the neutral species ScCl, TiCl, VCl, and CrCl whereas in section 8 we refer to the results on the charged species $MCl^{\pm}$; in section 9 we recapitulate our findings.

* Corresponding author. E-mail: mavridis@chem.uoa.gr.

2. Basis Sets and Methods

For the metal atoms, Sc−Cr, the correlation consistent basis sets of quadruple and quintuple cardinality by Balabanov and Peterson[6] were employed, combined with the corresponding augmented basis sets by Dunning and co-workers for the Cl atom.[7a] Both sets were generally contracted to [8s7p5d3f2g1h/$_M$ 7s6p4d3f2g/$_{Cl}$] = 4Z and [9s8p6d4f3g2h1i/$_M$ 8s7p5d4f3g2h/$_{Cl}$] = 5Z, comprising 188 and 284 spherical Gaussians, respectively. The 4Z basis set was used for the construction of all PECs of the neutral MCl molecules, while the 5Z for the ground and first excited-state of the MCls and the construction of the PECs of the anions (MCl^-), as well as in the study of the cations (MCl^+) around equilibrium. To study the effects of the $3s^23p^6$ semicore electrons of the metal atoms, the 4Z and 5Z basis sets were extended by a series of weighted core functions 2s+2p+2d+1f+1g+1h (= C4Z) and 2s+2p+2d+1f+1g+1h+1i (=C5Z),[6] giving rise to 233 and 342 one-electron spaces, respectively. The C4Z basis was further augmented by a series of Cl-weighted core functions, namely, 3s+3p+3d+2f+1g, to examine the core-correlation effects of the Cl atom.[7b] This basis set, generally contracted to [10s9p7d4f3g2h/$_M$ 10s9p7d5f3g/$_{Cl}$] ≡ $C^2$4Z, comprises 283 Gaussians. The large C4Z, C5Z, and $C^2$4Z basis sets were used only for the neutral MCl species and only for certain states.

Scalar relativistic effects for the neutrals only were estimated by the second-order Douglas−Kroll−Hess (DKH2) approach[8,9] using the 4Z, 5Z, and C4Z basis sets, but recontracted accordingly.[6,10]

Two calculational methodologies were followed in general: the complete active space self-consistent field (CASSCF) + single + double replacements (CASSCF+1 + 2=MRCI), and the restricted coupled-cluster + singles + doubles + quasi-perturbative connected triples [RCCSD(T)] method.[11] The zeroth-order multireference wave functions (CASSCF) are defined by alloting the valence 4s and 3d electrons of the metal + the $3p_z$ electron of the Cl atom to the 4s+3d+4p_z(M)+3p_z(Cl) orbitals, that is, 5, 6, and 7 e^- to 8 orbital functions for the TiCl, VCl, and CrCl molecules, respectively; see also ref 3. In ScCl we were forced to use all three 4p functions of Sc, and thus 4 e^- are distributed to 10 orbitals; the same procedure was followed for the cations, MCl^+. Valence internally contracted (ic)[12] MRCI wave functions are obtained through single and double excitations out of the reference functions, but including

10.1021/jp901225y CCC: $40.75 © 2009 American Chemical Society
Published on Web 05/20/2009

TABLE 1: Ionization Energies (IE, eV) and Energy Separations (cm^{-1}) of the First Excited State of Sc^+, Ti^+, V^+, and Cr^+ in Different Levels of Theory

	Sc	Sc^+	Ti	Ti^+	V	V^+	Cr	Cr^+
method/basis set[a]	IE	$^1D \leftarrow {}^3D$	IE	$^4F \leftarrow {}^4F$	IE	$^5D \leftarrow {}^5F$	IE	$^6D \leftarrow {}^6S$
MRCI/4Z	6.388	2067	6.707	985	6.566	2905	6.572	12623
MRCI+*Q*	6.394		6.708	905	6.531	3278	6.472	13928
C-MRCI/C4Z	6.441	2630	6.716	211	6.536	2882	6.679	11064
C-MRCI+*Q*	6.518	2373	6.727	289	6.494	3502	6.547	13390
MRCI+DKH2/4Z	6.421	2162	6.747	2477	6.837	1121	6.685	10490
MRCI+DKH2+*Q*	6.426		6.749	2396	6.803	1494	6.591	11786
C-MRCI+DKH2/C4Z	6.472	2718	6.758	1735	6.811	1062	6.794	8946
C-MRCI+DKH2+*Q*	6.549	2472	6.772	1816	6.774	1667	6.671	11159
MRCI/5Z	6.393	2033	6.714	952	6.574	2942	6.584	12633
MRCI+*Q*	6.398		6.716	871	6.538	3316	6.489	13939
C-MRCI/C5Z	6.441	2630	6.721	45	6.524	3052	6.683	11262
C-MRCI+*Q*	6.518	2382	6.734	88	6.483	3656	6.557	13503
RCCSD(T)/4Z	6.366		6.639	1089	6.492	3123	6.461	13732
C-RCCSD(T)/C4Z	6.500		6.751	−105	6.474	3993	6.632	13916
RCCSD(T)+DKH2/4Z	6.399		6.681	2581	6.773	1277	6.583	11564
C-RCCSD(T)+DKH2/C4Z	6.534		6.794	1425	6.753	2166	6.756	11731
expt[b]	6.5615	2444.45	6.8281	1085.44	6.7462	2719.89	6.7665	12277.87

[a] +*Q* refers to the Davidson correction; C- means that the $3s^23p^6$ electrons have been included in the CI procedure. [b] Reference 16.

of course the "complete" valence space of Cl (3s3p) for all neutrals and their cations. To take into account core-correlation for certain low-lying states of the MCls, the $3s^23p^6$ (M) electrons were included in the MRCI or RCCSD(T) procedures, tagged C-MRCI and C-RCCSD(T). In addition, for the ground and first excited state of the neutral species, RCCSD(T) calculations were performed by including both the $3s^23p^6$ (M) and the $2s^22p^6$ (Cl) semicore electrons [C^2-RCCSD(T)]. All calculations were performed under C_{2v} constraints.

Basis set superposition errors (BSSE), calculated as usual[13] at the MRCI/4Z (C-MRCI/C4Z) [RCCSD(T)/4Z] {C-RCCSD(T)/C4Z} level, are 0.21 (0.40) [0.23] {0.36}, 0.20 (0.21) [0.22] {0.31}, 0.18 (0.24) [0.25] {0.33}, and 0.26 (0.26) [0.36] {0.42} kcal/mol for the X-states of ScCl, TiCl, VCl, and CrCl, respectively. Using the 5Z basis set, BSSEs are significantly smaller, and therefore will not be considered any further.

Size nonextensivity (SNE) is one of the most pernicious problems of the CI-based methods. It can be estimated by subtracting the sum of the energies of the separated atoms from the total energy of the corresponding supermolecule ($r_{M-X} \approx$ 200 bohr) at the same level of theory. Using this approach, the SNE for the ground states of ScCl, TiCl, VCl, and CrCl are 2.0 (0.5), 11 (4.7), 13 (6.2), and 14 (3.6) mE_h at the MRCI(+*Q*)/4Z level of theory; corresponding MRCI(+*Q*)/5Z values are 1.9 (0.2), 12 (4.2), 15 (4.6), and 15 (4.4) mE_h, respectively. C-MRCI (+*Q*)/C4Z SNE values are as expected larger, specifically, 30 (8), 34 (11), 35 (11), and 40 (32) mE_h, respectively.

All calculations were performed by the MOLPRO suite of codes;[14] in certain cases the ACESII package was also employed.[15]

3. The Atoms

Table 1 lists ionization energies (IE) of the M atoms and energy differences between the ground and first excited state of M^+, M = Sc, Ti, V, and Cr. Similarly to MFs,[3,4] MCls are of ionic character with more than 0.6 e^- transferred from M to Cl and about 0.4 e^- from M^+ to Cl in the case of $MCls^+$ (vide infra). Therefore, low-lying states of the MCl and MCl^+ systems can be understood as stemming from the M^+ and M^{2+} atomic terms in the electric field of the spherical $Cl^-(^1S)$ anion. Within this context, Table 1 is useful showing our ability to calculate IEs and energy separations of the M^+ states (see also ref 6b), obviously related to the M^+Cl^- bonding model. At all levels of theory, IEs are in good agreement with experiment; in particular at the C-RCCSD(T)+DKH2/4Z level differences between theory and experiment do not exceed 0.03 eV, amounting to less than 0.5%. The situation changes, however, when we try to calculate energy separations between the ground and first excited state of the M^+ cations, $\Delta E(M^+)$. Remarkably enough, the best results are obtained at the "simple" MRCI/4Z level because of error cancelation. In particular the error at this level of theory, i.e., $\varepsilon = [1 - (\Delta E_{calc}(M^+))/(\Delta E_{expt}(M^+)^{16})] \times 100$ is 15, 9, −7, and −3% for Sc^+, Ti^+, V^+, and Cr^+, respectively. Practically the same percentage errors are obtained at the MRCI/5Z level. However, as the level of calculation increases, the absolute errors $|\varepsilon|$ increase with the exception of Sc^+. For instance, at the C-MRCI+DKH2+*Q* [C-RCCSD(T)+DKH2]/C4Z level, $|\varepsilon|$ = 1, 67 [31], 39 [20], and 9 [4], showing clearly the difficulties that one encounters with the 3d transition metals.

The experimental electron affinity (EA) of the chlorine atom is 3.612 724 ± 0.000 027 eV.[17] It is interesting to report the calculated values of EA obtained at different levels of CC theory, namely, RCCSD(T)/4Z (5Z), C-RCCSD(T)/C4Z (C5Z), RCCSD(T)+DKH2/4Z (5Z), and C-RCCSD(T)+DKH2/C4Z (C5Z): EA = 3.613 (3.640), 3.612 (3.641), 3.599 (3.626), and 3.597 (3.624) eV, respectively. Observe the almost perfect agreement with experiment at the RCCSD(T)/4Z level which of course is accidental. As expected, MRCI(+*Q*) EAs are less accurate, i.e., 3.404 (3.540) and 3.426 (3.564) eV employing the 4Z and 5Z basis sets, respectively.

4. Results and Discussion on ScCl

Relevant experimental work on ScCl is presented in Table 2 according to refs 18−22; no accurate experimental dissociation energy (D_e) exists for ScCl in the literature. A value of D_0 = 3.4 eV (=78.4 kcal/mol) given in the Huber−Herzberg compilation[22] is obtained by the approximate formula $D_e = (\omega_e^2)/(4\omega_e x_e)$, whereas a D_e = 3.55 eV (=81.9 kcal/mol) obtained through the same formula is given in ref 21. A much larger D_0 value of at least 120 kcal/mol is suggested by deBlasi Bourdon and Prince obtained by thermochemical analysis.[23]

The first ab initio work on ScCl appeared 20 years ago by Langhoff et al.[24] who studied the isovalent series MX (M = Sc, Y; X = F, Cl, Br). For ScCl they studied the $X\ ^1\Sigma^+$ and a

TABLE 2: Experimental Results on $Sc^{35}Cl$: Bond Distances r_e (Å), Harmonic and Anharmonic Frequencies ω_e (cm^{-1}) and $\omega_e x_e$ (cm^{-1}), Rotational Vibrational Constants α_e (cm^{-1}), Centrifugal Distortions $\bar{D}_e$ (cm^{-1}), and Energy Separations T_e or T_{00} (cm^{-1}) from the X-State[j]

state	r_e	ω_e	$\omega_e x_e$	$\alpha_e \times 10^3$	$\bar{D}_e \times 10^7$	T_{00}
X $^1\Sigma^+$[a]	2.23026	447.523	1.67025	0.8681	1.0289	0.0
X $^1\Sigma^+$[b]	2.23025	440.665	1.6137	0.828	0.9678	
X $^1\Sigma^+$[c]					1.03005	
X $^1\Sigma^+$[d]	2.23028928(95)	445.1(26)	1.714(30)	0.8684		
a $^3\Delta_2$ (1)[a]	2.323	398.3	1.36		1.0336	x[e]
b $^3\Pi_0$ (1)[a,f]	2.344				1.02	3429.05
A Δ(1)[a]	2.337	388.09		0.707	1.00	3555.741(T_e)
c $^3\Sigma^+$ (1)[a]	2.3475	367.712	1.2983	0.81178	1.113	5385.043(T_e)
B $^1\Pi$ (1)[a]	2.3506	381.793	1.3725	0.7882	1.03	6020.539(T_e)
C $^1\Sigma^+$ (2)[a]	2.3305	377.59	1.42	0.7904	1.107	12427.456(T_e)
C $^1\Sigma^+$ (2)[g]	2.333	373.9	0.9	0.7904	1.1	12431.2(T_e)
$^3\Phi_3$ (1)[a]	2.380				1.123	12564.37+x
$^3\Delta_2$ (2)[a]	2.372	355.9	2.18		1.112	13088.60+x
D $^1\Pi$ (2)[a,h]	2.348	374.3	2.3		1.1	17390.06
D $^1\Pi$ (2)[c]					1.1011	17574.6914(15)
$^1\Phi$(1)[a]	2.328				1.99	20267.478
$^1\Delta$ (2)[a]	2.355				1.00	20342.7
$^1\Delta$(3)[a]	2.354	376.39	2.02	0.996	1.02	21121.63(T_e)
$^1\Pi$ (3)[a,h]	2.337	374.19	2.1	0.829	1.25	21518.9(T_e)
$^1\Sigma^+$(3)[a,i]	2.372				0.919	22431.76

[a] Reference 18. [b] Isotopomer $Sc^{37}Cl$, ref 19. [c] Reference 20. [d] Reference 21 [e] $x \approx 1000$ cm^{-1} from ref 18. [f] The $\Omega = 0$ value of the b $^3\Pi$ (1) state is characterized as "uncertain". [g] Tagged as "A $^1\Sigma^+$" in ref 22. [h] For the D $^1\Pi$ (2), $^1\Pi$ (3) states $T_e = 17613.3$, 21521.1 cm^{-1}, respectively, according to ref 22. [i] Isotopomer $Sc^{37}Cl$. [j] Nine more excited states located higher than 21500 cm^{-1} from the X $^1\Sigma^+$ state are listed in Huber and Herzberg compilation,[22] namely (T_e in parentheses): $^1\Sigma^+$ (27033.3), $^1\Pi$ (31249.9), $^3\Delta$(a=unknown), $^3\Phi$(12567.6+a=T_{00}), $^3\Delta$(13113.8+a), $^3\Sigma$ (d), $^3\Pi$ (22260.0+d), X (x'), y(27189+x').

$^3\Delta$ states around equilibrium at the CISD(+Q) and CPF + scalar relativistic effects (Cowan-Griffin) levels using a [8s6p4d3f/$_{Sc}$ 6s5p3d1f/$_{Cl}$] basis set, reporting r_e, ω_e, D_0, T_e, and μ_e (dipole moment). In 1996 Boutassetta et al.[25] published results (r_e, ω_e, $\omega_e x_e$, T_e) for five low-lying states of ScCl around equilibrium at the valence MRCI+Q/[8s6p4d3f/$_{Sc}$ 7s5p2d/$_{Cl}$] level using a truncated CASSCF reference function. Finally, Taher-Mansour et al.[26] examined a series of 18 states of ScCl around equilibrium at the MRCI+Q/[8s6p4d3f/$_{Sc}$ 7s5p2d/$_{Cl}$] level of theory, reporting r_e, ω_e, and T_e values.

The ground state of Sc^+ is $^3D(4s^13d^1)$ with its first five excited states $^1D(4s^13d^1)$, $^3F(3d^2)$, $^1D(3d^2)$, $^1S(4s^2)$, and $^3P(3d^2)$ located 2444.45, 4812.52, 10848.06, 11639.86, and 12031.34 cm^{-1} higher, respectively.[16] In the static electric field of $Cl^-(^1S)$ the terms above give rise to 16 molecular $^{2S+1}|\Lambda|$states, namely [$^3\Sigma^+$, $^3\Pi$, $^3\Delta$], [$^1\Sigma^+$, $^1\Pi$, $^1\Delta$], [$^3\Sigma^-$, $^3\Pi$, $^3\Delta$, $^3\Phi$], [$^1\Sigma^+$, $^1\Pi$, $^1\Delta$], [$^1\Sigma^+$], and [$^3\Sigma^-$, $^3\Pi$], respectively. We have constructed MRCI/4Z PECs for all these states but one ($^1\Sigma^+$), spanning an energy range of 3.2 eV. A second $^3\Phi(2)$ and a fourth $^3\Pi(4)$ state have also been computed correlating to $Sc(^4F^0;3d^14s^14p^1)$ and $Sc(^4F^0)$ or $Sc(^4D^0;3d^14s^14p^1)$, respectively. All 17 states are bound at the MRCI/4Z level of theory with respect to adiabatic neutral fragments Sc + $Cl(^2P)$, and with respect to ground-state atoms $Sc(^2D)$ + $Cl(^2P)$. In addition, four more quintet states of repulsive character have been calculated, namely, $^5\Sigma^-$, $^5\Pi$, $^5\Delta$, and $^5\Phi$ about 50 000 cm^{-1} above the X-state, all correlating to the first excited state of $Sc(^4F;\ 3d^24s^1)$ + $Cl(^2P;\ M_L=0)$. At the MRCI+Q/4Z level their PECs show van der Waals minima of 47, 50, 54, and 27 cm^{-1}, respectively, at about 5.4−5.5 Å. The PECs of the 21 examined states are displayed in Figures 1 and 2, whereas Table 3 lists our numerical findings along with experimental results for easy comparison.

A. States X $^1\Sigma^+$, a $^3\Delta$(1), A $^1\Delta$(1), b $^3\Pi$(1), c $^3\Sigma^+$(1), and B $^1\Pi$(1). As it was already mentioned, the X $^1\Sigma^+$, B$^1\Pi$(1), A $^1\Delta$(1) and c $^3\Sigma^+$(1), b $^3\Pi$(1), a $^3\Delta$(1) states correlate diabatically to $Sc^+(^1D;\ 4s^13d^1)$ and $Sc^+(^3D;\ 4s^13d^1)$ + $Cl^-(^1S)$, respectively.

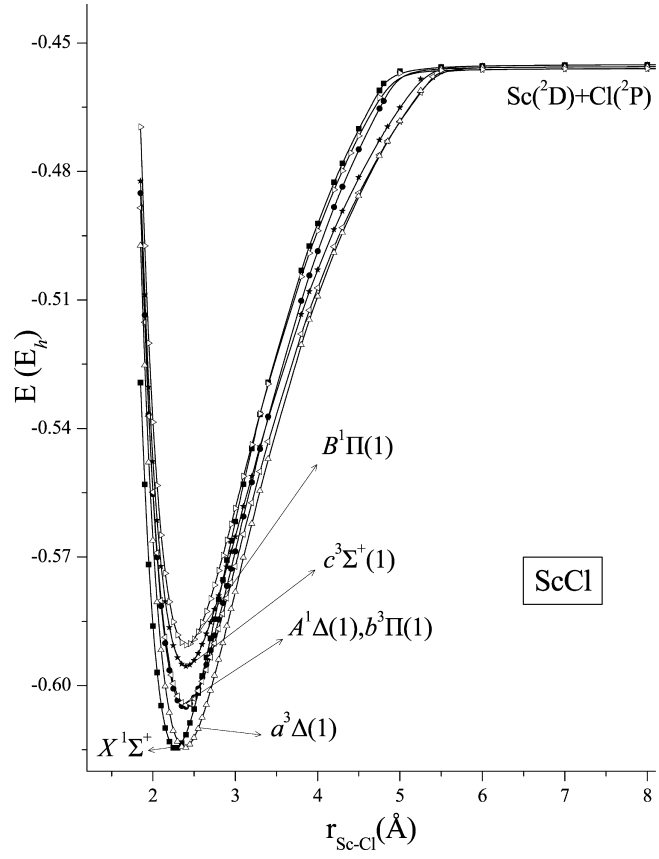

Figure 1. MRCI/4Z potential energy curves of the X $^1\Sigma^+$ and first five excited states of ScCl. Energies are shifted by +1219 E_h.

Adiabatically, however, they all correlate to the ground-state neutral atoms $Sc(^2D)$ + $Cl(^2P)$ due to avoided crossings at 5.5 (triplets) and 5.0 Å (singlets); see Figure 1. According to the experimentalists, the ground state is of $^1\Sigma^+$ symmetry with a $^3\Delta$ state about 1000 cm^{-1} higher.[18] Our results corroborate

the experimental results, although we were unable to determine an accurate a $^3\Delta-X\ ^1\Sigma^+$ splitting (but see below). Interestingly, these six states above are grouped in three mutual near degenerate pairs, [X $^1\Sigma^+$, a $^3\Delta(1)$], [A$^1\Delta(1)$, b $^3\Pi(1)$], and [c $^3\Sigma^+(1)$, B $^1\Pi(1)$].

The leading equilibrium MRCI/4Z configurations of the first six lowest states and their Mulliken atomic populations are as follows [the 28 "core" electrons $1s^22s^22p^63s^23p^6/_{Sc}$ $1s^22s^22p^6/_{Cl}$ are suppressed counting only the 10 "valence" electrons, 3 on Sc + 7 on Cl.

$$|X^1\Sigma^+\rangle_{A_1} \approx |1\sigma^2 2\sigma^2[(0.80)3\sigma^2 - (0.44)3\sigma^2 4\bar{\sigma}^1]1\pi_x^1 1\pi_y^2\rangle$$

$$4s^{1.37}4p_z^{0.18}4p_{x,y}^{0.12}3d_{z^2}^{0.58}3d_{xz}^{0.08}3d_{yz}^{0.08}3d_{x^2-y^2}^{0.01}3d_{xy}^{0.01}/ \quad 3s^{1.97}3p_z^{1.71}3p_x^{1.86}3p_y^{1.86}$$

$$|a^3\Delta(1)\rangle_{A_1} \approx 0.95|1\sigma^2 2\sigma^2 3\sigma^1 1\pi_x^2 1\pi_y^2 1\delta_+^1\rangle$$

$$4s^{0.85}4p_z^{0.23}4p_{x,y}^{0.04}3d_{z^2}^{0.11}3d_{xz}^{0.05}3d_{yz}^{0.05}3d_{x^2-y^2}^{1.00}/3s^{1.98}3p_z^{1.76}3p_x^{1.89} \times 3p_y^{1.89}$$

$$|A^1\Delta(1)\rangle_{A_1} \approx 0.92|1\sigma^2 2\sigma^2 3\sigma^1 1\pi_x^2 1\pi_y^2 1\bar{\delta}_+^1\rangle$$

$$4s^{0.80}4p_z^{0.27}4p_{x,y}^{0.08}3d_{z^2}^{0.10}3d_{xz}^{0.05}3d_{yz}^{0.05}3d_{x^2-y^2}^{0.97}/3s^{1.98}3p_z^{1.76}3p_x^{1.89} \times 3p_y^{1.89}$$

$$|b^3\Pi(1)\rangle_{B_1} \approx 0.95|1\sigma^2 2\sigma^2 3\sigma^1 1\pi_x^2 1\pi_y^2 2\pi_x^1\rangle$$

$$4s^{0.85}4p_z^{0.22}4p_{x,y}^{0.07}3d_{z^2}^{0.11}3d_{xz}^{0.99}3d_{yz}^{0.05}/3s^{1.99}3p_z^{1.76}3p_x^{1.90}3p_y^{1.90}$$

$$|c^3\Sigma^+(1)\rangle_{A_1} \approx 0.95|1\sigma^2 2\sigma^2 3\sigma^1 4\sigma^1 1\pi_x^2 1\pi_y^2\rangle$$

$$4s^{0.86}4p_z^{0.34}4p_{x,y}^{0.04}3d_{z^2}^{0.96}3d_{xz}^{0.05}3d_{yz}^{0.05}/3s^{1.98}3p_z^{1.78}3p_x^{1.88}3p_y^{1.88}$$

$$|B^1\Pi(1)\rangle_{B_1} \approx 0.93|1\sigma^2 2\sigma^2 3\sigma^1 1\pi_x^2 1\pi_y^2 2\bar{\pi}_x^1\rangle$$

$$4s^{0.83}4p_z^{0.18}4p_{x,y}^{0.07}3d_{z^2}^{0.14}3d_{xz}^{0.97}3d_{yz}^{0.06}3d_{x^2-y^2}^{0.02}3d_{xy}^{0.02}/3s^{1.99}3p_z^{1.76} \times 3p_x^{1.90}3p_y^{1.90}$$

For all states above about 0.6−0.7 e^- are transferred from Sc to Cl. Observe the constancy of the in situ populations of chlorine reflecting its ionic character. Henceforth, chlorine populations will be also suppressed and denoted simply as $Cl^{\delta-}$ giving only the value of δ. Adopting the ionic picture Sc^+Cl^-, the structure of ScCl can be described by the following vbL (valence-bond Lewis) diagram.

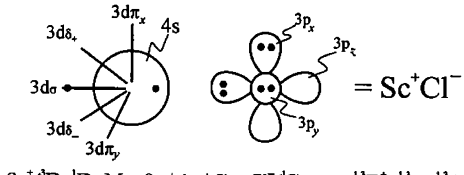

Moving the symmetry defining 3d electron on the metal from 3dσ ($M_L = 0$) to 3dπ_x or 3dπ_y ($M_L = \pm1$), to 3dδ_+ or 3dδ_- ($M_L = \pm2$) one obtains the Σ, Π, and Δ states, singlets, or triplets.

We describe now in some detail the X $^1\Sigma^+$ state. According to Table 3, as the level of the (valence) MRCI increases from MRCI(+Q)/4Z to MRCI(+Q)/5Z to MRCI+DKH2(+Q)/4Z, the binding increases monotonically from D_e = 100.1 (103.8) to 102.6 (105.6) to 103.4 (106.1) kcal/mol. Assuming additivity of the scalar relativistic effects, 3.3 (2.3) kcal/mol, our MRCI(+Q)/

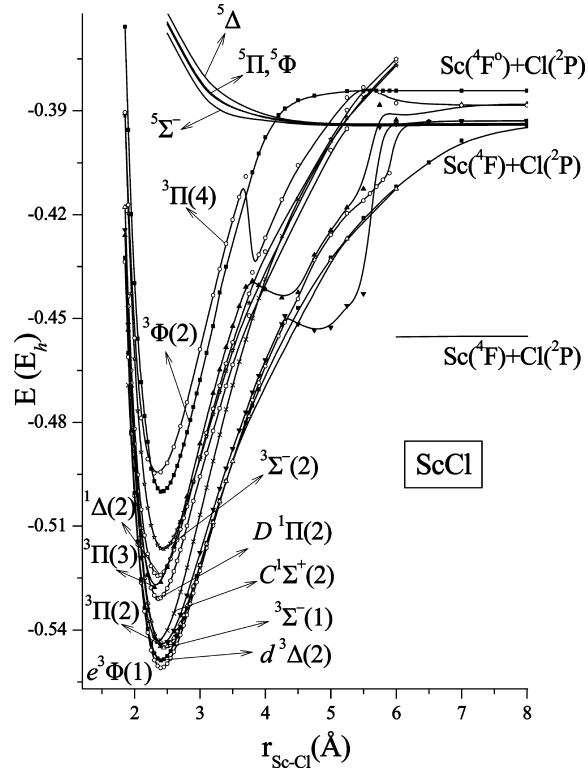

Figure 2. MRCI/4Z potential energy curves of the higher excited states of ScCl. Energies are shifted by +1219 E_h.

5Z+relativity(4Z) D_e is estimated to be 105.9 (107.9) kcal/mol. Including the core effects of Sc ($3s^23p^6$), the D_e value decreases, but at the MRCI level (C-MRCI) the results are not very reliable due to large size-nonextensivity effects, although they are consistent in sign with the coupled-cluster values (vide infra). Therefore, disregarding core MRCI effects, our suggested D_e MRCI value is 108 kcal/mol. Following on the other hand the CC sequence, that is RCCSD(T)/4Z, RCCSD(T)/5Z, C-RCCSD(T)/C4Z, C-RCCSD(T)/C5Z, we obtain D_e = 104.5, 105.4, 103.4, 104.3 kcal/mol, respectively. Observe that core effects on Sc decrease the binding energy by 1.1 kcal/mol at both C4Z and C5Z levels; by adding, however, the $2s^22p^6$ electrons of Cl, the C^2-RCCSD(T)/$C^2$4Z D_e increases by 0.5 kcal/mol. Therefore, we can claim that the total core effects of both Sc and Cl is a mere decrease of D_e by 0.6 kcal/mol. Relativistic effects, RCCSD(T)+DKH2/4Z [C-RCCSD(T)+DKH2/C4Z], add another 1.4 [1.2] kcal/mol to D_e. Taking everything into account, C-RCCSD(T)/C5Z + relativity(C4Z) + core(Cl/$C^2$4Z), we get D_e = 104.3 + 1.2 + 0.5 = 106 kcal/mol, in good agreement with the MRCI result of 108 kcal/mol. Recall that core effects were not taken into account at the MRCI level, but we know for certain that they should decrease slightly the binding energy. Thus our recommended dissociation energy of the X $^1\Sigma^+$ of ScCl is D_e = 107 ± 1 kcal/mol, suggesting that the thermochemical value (lower limit) of ∼120 kcal/mol[23] is perhaps overestimated.

From the above discussion it is clear that core + relativistic effects combined do not play any significant role on the D_e value of the ScCl system. Observe that the "plain" MRCI+Q/5Z and RCCSD(T)/5Z D_e values are 105.6 and 105.4 kcal/mol, respectively; Table 3.

Concerning now the bond distance of X $^1\Sigma^+$ state at all levels of theory, (valence) MRCI or CC, the r_e is very close to 2.270 Å about 0.04 Å larger than the experimental one. The effect mainly of the $3s^23p^6$ core electrons of Sc is what brings the

TABLE 3: Total Energies E (E_h), Dissociation Energies D_e (kcal/mol), Bond Distances r_e (Å), Harmonic and Anharmonic Frequencies ω_e, $\omega_e x_e$ (cm^{-1}), Rotational−Vibrational Constants α_e (cm^{-1}), Centrifugal Distortions $\bar{D}_e$ (cm^{-1}), Dipole Moments μ_e (D), and Energy Separations T_e (cm^{-1}) of $Sc^{35}Cl$

method/basis set[a]	−E	D_e	r_e	ω_e	$\omega_e x_e$	$\alpha_e \times 10^3$	$\bar{D}_e \times 10^7$	$\langle\mu\rangle$ (μ_{FF})[b]	T_e
				X $^1\Sigma^+$					
MRCI/4Z	1219.614681	100.1	2.276	434	1.67	0.848	0.963	2.35 (2.69)	0.0
MRCI+*Q*	1219.636782	103.8	2.270	438	1.67	0.842	0.960	... (2.49)	0.0
C-MRCI/C4Z	1219.905251	96.6	2.251	431				2.27 (2.90)	0.0
C-MRCI+*Q*	1219.971471	101.1	2.242	420					0.0
MRCI+DKH2/4Z	1224.577490	103.4	2.275	439				2.30 (2.54)	0.0
MRCI+DKH2+*Q*	1224.598093	106.1	2.273	441					0.0
C-MRCI+DKH2/C4Z	1224.866497	99.1	2.252	435				2.22 (3.03)	0.0
C-MRCI+DKH2+*Q*	1224.930619	102.3	2.244	430					0.0
MRCI/5Z	1219.625039	102.6	2.275	436	1.99	0.778	0.953	2.48 (2.64)	0.0
MRCI+*Q*	1219.646233	105.6	2.272	437	1.51	0.829	1.078		0.0
C-MRCI/C5Z	1219.918938	98.5	2.254	439				2.40 (3.25)	0.0
C-MRCI+*Q*	1219.984346	102.6	2.245	435					0.0
RCCSD(T)/4Z	1219.640690	104.5	2.271	439	1.67	0.812	0.956	... (2.39)	0.0
C-RCCSD(T)/C4Z	1219.987807	103.4	2.236	447	1.67	0.876	1.009	... (2.80)	0.0
C^2-RCCSD(T)/$C^2$4Z	1220.326863	103.9	2.232	448	1.44	0.882	0.997	... (2.75)	0.0
RCCSD(T)+DKH2/4Z	1224.600196	105.9	2.269	440				... (2.29)	0.0
C-RCCSD(T)+DKH2/C4Z	1224.946669	104.6	2.234	443				... (2.59)	0.0
RCCSD(T)/5Z	1219.648445	105.4	2.269	444				... (2.41)	0.0
C-RCCSD(T)/C5Z	1220.001003	104.3	2.233	448	1.69	0.864	1.009	... (2.74)	0.0
$8e^-$ CPF+Rel[c]		105.5	2.266	434				2.623[d]	
expt		~120[e]	2.23026[f]	447.523[f]	1.67025[f]	0.8681[f]	1.0289[f]		
			2.23028928(95)[g]	445.1(26)[g]	1.714(30)[g]	0.8684[g]			
				a $^3\Delta$(1)					
MRCI/4Z	1219.614564	99.8	2.381	383	1.35	0.760	0.939	3.35 (3.66)	26
MRCI+*Q*	1219.634224	102.0	2.378	383	1.35	0.764	0.946	... (3.81)	561
C-MRCI/C4Z	1219.908397	98.4	2.351	397				3.16 (3.71)	−690
C-MRCI+*Q*	1219.971429	101.1	2.344	392					9.2
MRCI+DKH2/4Z	1224.570917	98.9	2.380	384				3.45 (3.76)	1443
MRCI+DKH2+*Q*	1224.590355	101.0	2.378	379					1698
C-MRCI+DKH2/C4Z	1224.864641	97.6	2.349	377				3.24 (3.81)	408
C-MRCI+DKH2+*Q*	1224.926891	100.3	2.338	369					818
MRCI/5Z	1219.622328	100.9	2.380	383	1.33	0.895	0.943	3.39 (3.74)	595
MRCI+*Q*	1219.642240	103.1	2.377	384	1.24	0.641	0.946		876
C-MRCI/C5Z	1219.920832	99.7	2.349	390				3.33 (3.81)	−416
C-MRCI+*Q*	1219.984954	103.0	2.336	384					−133
RCCSD(T)/4Z	1219.637304	102.4	2.376	384	1.35	0.771	0.953	... (3.71)	743
C-RCCSD(T)/C4Z	1219.987198	103.2	2.333	396	1.40	0.789	0.999	... (3.81)	134
C^2-RCCSD(T)/$C^2$4Z	1220.326132	103.5	2.330	398	1.37	0.799	0.996	... (3.81)	160
RCCSD(T)+DKH2/4Z	1224.592733	101.2	2.375	376				... (3.76)	1638
C-RCCSD(T)+DKH2/C4Z	1224.942403	101.9	2.332	428				... (3.82)	936
RCCSD(T)/5Z	1219.644935	103.2	2.374	389				... (3.72)	770
C-RCCSD(T)/C5Z	1220.000692	104.1	2.330	382				... (3.80)	68
$8e^-$ CPF+Rel[c]			2.368	382				3.881[d]	1226
expt[f]			2.323	398.3	1.36		1.0336		~1000
				A $^1\Delta$(1)					
MRCI/4Z	1219.605018	93.8	2.385	384	1.29	0.750	0.930	2.51 (2.64)	2121
MRCI+*Q*	1219.624433	95.8	2.384	383	1.37	0.752	0.935	... (2.64)	2710
C-MRCI/C4Z	1219.898046	91.8	2.355	409				2.32 (2.59)	1581
C-MRCI+*Q*	1219.960690	94.3	2.347	405					2366
MRCI/5Z	1219.611965	94.4	2.384	387				2.49 (2.63)	2869
MRCI+*Q*	1219.631983	96.6	2.383	385					3127
expt[f]			2.337	388.09		0.707	1.00		3555.741
				b $^3\Pi$(1)					
MRCI/4Z	1219.604565	93.2	2.402	367	1.30	0.746	0.973	3.50 (3.66)	2220
MRCI+*Q*	1219.624631	95.8	2.395	368	1.29	0.746	0.983	... (3.51)	2667
C-MRCI/C4Z	1219.897484	91.4	2.375	373				3.32 (3.77)	1705
C-MRCI+*Q*	1219.960419	94.5	2.364	376					2426
MRCI/5Z	1219.611485	94.1	2.400	370				3.41 (3.60)	2975
MRCI+*Q*	1219.631857	96.6	2.395	367					3155
expt[f]			2.344				1.02		3429.05 (T_{00})
				c $^3\Sigma^+$(1)					
MRCI/4Z	1219.595529	88.1	2.403	356	1.35	0.790	1.077	2.49 (2.49)	4203
MRCI+*Q*	1219.615932	90.7	2.397	356	1.25	0.783	1.050	... (2.34)	4576
C-MRCI/C4Z	1219.887607	85.5	2.380	364				2.43 (2.54)	3872
C-MRCI+*Q*	1219.951395	88.6	2.368	358					4406

TABLE 3: Continued

method/basis set[a]	$-E$	D_e	r_e	ω_e	$\omega_e x_e$	$\alpha_e \times 10^3$	$\bar{D}_e \times 10^7$	$\langle\mu\rangle$ (μ_{FF})[b]	T_e
MRCI/5Z	1219.602204	88.9	2.401	378				2.48 (2.46)	5012
MRCI+Q	1219.623127	91.5	2.395	375					5071
expt[f]			2.3475	367.712	1.2983	0.81178	1.113		5385.043
				B $^1\Pi$(1)					
MRCI/4Z	1219.590578	84.4	2.406	368	1.39	0.754	0.957	4.17 (4.37)	5290
MRCI+Q	1219.611284	87.5	2.402	369	1.32	0.759	0.965	... (4.37)	5596
C-MRCI/C4Z	1219.881964	81.6	2.386	378				3.91 (4.47)	5111
C-MRCI+Q	1219.945660	85.2	2.375	371					5665
MRCI/5Z	1219.597195	85.1	2.410	398				4.06 (4.44)	6111
MRCI+Q	1219.618673	88.3	2.405	395					6049
expt[f]			2.3506	381.793	1.3725	0.7882	1.03		6020.539
				d $^3\Delta$(2)					
MRCI/4Z	1219.548793	97.1	2.406	348	1.64	0.866	1.074	6.50 (5.41)	14421
MRCI+Q	1219.572096	100.7	2.400	351	1.44	0.883	1.070		14197
C-MRCI/C4Z	1219.847655		2.397	343		0.872	1.129	6.27 (5.47)	12641
C-MRCI+Q	1219.913573		2.388	352			1.156		12707
expt[f]			2.372	355.9	2.18	1.112			13088.60+x[h]
				e $^3\Phi$(1)					
MRCI/4Z	1219.547921	97.3	2.437	335	1.31	0.785	1.074	7.13 (6.71)	14562
MRCI+Q	1219.570530	99.9	2.427	339	1.31	0.796	1.072		14541
C-MRCI/C4Z	1219.848399		2.419	341	4.63	0.762	1.081	7.20 (6.83)	12478
C-MRCI+Q	1219.914115		2.408	337			1.140		12588
expt[f]			2.380				1.123		12564.37+x[h]
				$^3\Sigma^-$(1)					
MRCI/4Z	1219.545120	94.7	2.450	335	1.32	0.804	1.063	6.21 (6.25)	15267
MRCI+Q	1219.567283	97.8	2.437	340	1.33	0.835	1.041		15253
				C $^1\Sigma^+$(2)					
MRCI/4Z	1219.543268		2.356	371	1.23	0.795	1.068	4.62 (4.59)	15673
MRCI+Q	1219.573493		2.357	376	1.15	0.739	1.037		13890
C-MRCI/C4Z	1219.833848		2.346	365	1.10	0.834	1.132	4.11 (4.93)	15650
C-MRCI+Q	1219.898144		2.333	376	1.26	0.859	1.106		16093
expt[f]			2.3305	377.59	1.42	0.7904	1.107		12427.456
				$^3\Pi$(2)					
MRCI/4Z	1219.544452	95.2	2.416	346	1.51	0.896	1.053	5.34 (4.98)	15413
MRCI+Q	1219.567881	98.3	2.412	351	1.57	0.919	1.042		15122
				D $^1\Pi$(2)					
MRCI/4Z	1219.530917		2.366	384	1.56	0.827	0.960	3.35 (3.35)	18384
MRCI+Q	1219.552127		2.368	381	1.63	0.843	0.980		18579
expt[f]			2.348	374					17390.06
				$^3\Pi$(3)					
MRCI/4Z	1219.527677	87.6	2.313	419	2.61	0.934	0.925	2.90 (2.39)	19095
MRCI+Q	1219.553420	94.9	2.301	422	2.61	1.072	0.950		18296
				$^1\Delta$(2)					
MRCI/4Z	1219.524381		2.365	372	1.46	0.886	1.039	6.61 (5.60)	19819
MRCI+Q	1219.549479		2.362	376	1.50	0.860	1.027		19161
expt[e]			2.355				1.00		20342.7
				$^3\Sigma^-$(2)					
MRCI/4Z	1219.516660		2.434	344	1.34	0.798	1.057	7.35 (7.32)	21513
MRCI+Q	1219.542515		2.420	352	1.37	0.807	1.004		20689
				$^3\Phi$(2)					
MRCI/4Z	1219.499031	72.1	2.425	377	1.16	0.691	0.870	8.61 (8.23)	25382
MRCI+Q	1219.523615	75.0	2.412	382	1.30	0.674	0.874		24837
				$^3\Pi$(4)					
MRCI/4Z	1219.497302	68.4	2.336	383	2.60	1.004	1.033	8.33 (7.98)	25762
MRCI+Q	1219.522568	73.1	2.307	397	3.49	1.481	1.041		25067

[a] +Q refers to the Davidson correction; C- and C^2- means that the $3s^23p^6$ and $2s^22p^6$ electrons of Sc and Cl, respectively, have been included in the CI. [b] $\langle\mu\rangle$ calculated as an expectation value, μ_{FF} through the finite field approach; field strength 5×10^{-5} au. [c] Reference 24. Coupled pair functional calculations + scalar (Cowan-Griffin) relativistic effects; basis set [8s6p4d3f/$_{Sc}$ 6s5p3d1f/$_{Cl}$]. [d] Without relativistic corrections. [e] Reference 23, thermochemical data. [f] Reference 18, but see text. [g] Reference 21, microwave Fourier transform spectroscopy. [h] $x \approx 1000$ cm^{-1}; see ref 18.

calculated r_e in agreement with experiment. Specifically, at the C-RCCSD(T)/C5Z level $r_e = 2.233$ Å; adding to this the core effects of Cl [C^2-RCCSD(T)/$C^2$4Z] and of scalar relativity [C-RCCSD(T)+DKH2/C4Z], we get $r_e = 2.233 + (-0.004) + (-0.002) = 2.227$ Å, in very good agreement with the experimental value of 2.2303 Å.[18,21]

At the C-MRCI+Q/C5Z level r_e = 2.245 Å, in acceptable agreement with experiment considering the size nonextensivity of the MRCI method when dealing with a total of 18 electrons.

Finally, a few comments for the dipole moment (μ_e) of the X $^1\Sigma^+$ state are in order. Notice first that MRCI μ_e values obtained as expectation values $\langle\mu\rangle$ differ considerably from the corresponding finite-field ones, μ_{FF}, the latter being almost always larger. According to ref 27 the μ_{FF} is to be preferred. Disregarding the C-MRCI μ_e values, the MRCI/5Z dipole moment is μ_{FF} = 2.64 D; this value is diminished by 0.15 D due to relativistic effects (MRCI/4Z vs MRCI+DKH2/4Z), thus a μ_e = 2.5 D is predicted through the (valence) MRCI approach. The corresponding C-RCCSD(T)/C5Z value μ_{FF} = 2.74 D should be reduced by 0.21 D due to relativity [C-RCCSD(T)/C4Z vs C-RCCSD(T)+DKH2/C4Z], thus μ_e = 2.5 D, in agreement with the (valence) MRCI result.

We turn now to the a $^3\Delta(1)$ state lying slightly higher than the ground state X $^1\Sigma^+$. As Table 3 shows the T_e (a $^3\Delta-$X $^1\Sigma^+$) gap ranges from 1698 (MRCI+DKH2+Q/4Z) to −690 cm^{-1} (C-MRCI/C4Z), depending strongly on the method and basis set used. It is interesting what the experimentalists have to say in relation to the a $^3\Delta-$X $^1\Sigma^+$ splitting: "However, the energy of a $^3\Delta$ in ScCl remains to be experimentally determined", suggesting an estimated value of about 1000 cm^{-1} based on the ab initio results of Langhoff et al.,[24] and to the analogy with the experimental energy separations T_{00}(a $^3\Delta-$X $^1\Sigma^+$) of ScF[28] and ScI,[29] 1969.0 and 364.4 cm^{-1}, respectively. For a discussion on the a $^3\Delta-$X $^1\Sigma^+$ separation of ScF based on recent ab initio calculations, see also ref 5.

Based on the MRCI(+Q)/5Z results, T_e(a $^3\Delta-$X $^1\Sigma^+$) = 876 cm^{-1}; including core effects (C-MRCI+Q/C5Z) this order is formally reversed, the two states becoming in essence degenerate (T_e = −133 cm^{-1}). Adding scalar relativistic effects the X $^1\Sigma^+-$a $^3\Delta(1)$ ordering is strongly restored at both MRCI+DKH2(+Q)/4Z and C-MRCI+DKH2(+Q)/C4Z levels of theory.

Similar trends are obtained by the coupled-cluster method. At the RCCSD(T)/4Z,C-RCCSD(T)/C4Z [C^2-RCCSD(T)/C^{2}4Z] we get T_e = 743, 134 [160] cm^{-1}. RCCSD(T)+DKH2/4Z relativistic effects boost the a $^3\Delta(1)-$X $^1\Sigma^+$ difference to 1638 cm^{-1}, but adding core effects at the same level of theory, the energy separation decreases to 936 cm^{-1}. Assuming additivity of relativistic effects and core effects of Cl ($2s^22p^6$), a better estimate can be obtained from the relation T_e(a $^3\Delta-$X $^1\Sigma^+$) = C-RCCSD(T)/C5Z + core effects of Cl[C^2-RCCSD(T)/C^{2}4Z] + relativistic effects [C4Z] = 68 + (160 − 134) + (936 − 134) = 896 cm^{-1}, very close to the 876 cm^{-1} value at the MRCI+Q/5Z level, obviously due to cancelation of core and relativistic effects.

The discussion above shows that the ground state of ScCl is $^1\Sigma^+$ with the first excited state, a $^3\Delta$, located close to 1000 cm^{-1} higher, in agreement with the experimental estimate.[18]

Concerning now the bond distance of the a $^3\Delta(1)$ state and following the same line of approach, we obtain r_e = r_e[C-RCCSD(T)/C5Z] + core effects of Cl($2s^22p^6$) + relativistic effects [C-RCCSD(T)/C4Z] = 2.330 + (−0.003) + (−0.001) = 2.326 Å, in excellent agreement with the experimental value of 2.323 Å[18] The corresponding MRCI r_e value is as expected longer, namely, r_e = r_e[C-MRCI+Q/C5Z] + relativistic effects [C4Z] = 2.336 + (−0.006) = 2.330 Å.

Finally, the finite field dipole moment converges to μ_{FF}(a $^3\Delta$) = 3.8 D at both MRCI and CC methods.

Our findings indicate that core ($3s^23p^6$) + scalar relativistic effects combined seem to play a minor rôle concerning dissociation energies, energy separations, and even dipole moments. Core effects alone, responsible for a reduction of bond lengths of about 0.03 Å(MRCI), are instrumental in bringing into agreement theory and experiment. This holds true for the first six states where core effects have been taken into consideration at the MRCI level.

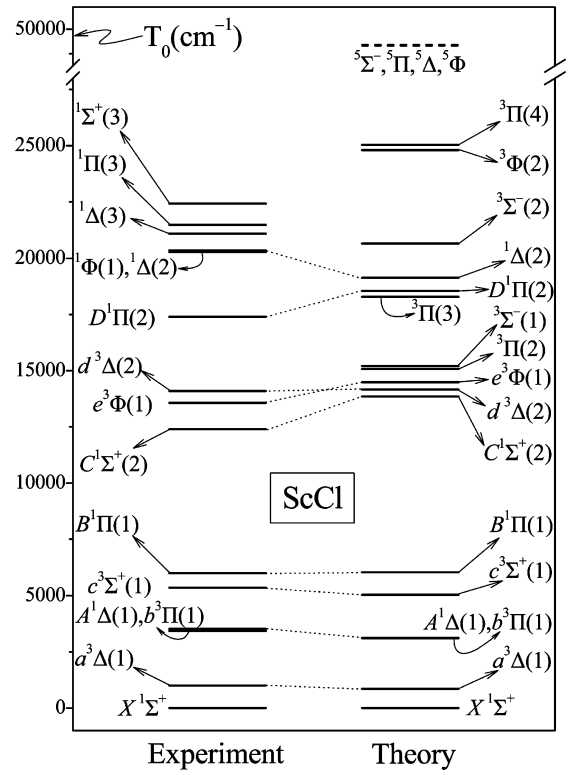

Figure 3. Comparative energy level diagram of experimentally determined vs theoretically predicted ScCl states. See text for details.

The experimental energy difference of the next pair of states, A $^1\Delta(1)$ and b $^3\Pi(1)$, is ∼100 cm^{-1}, with T_{00} values of 3526 and 3429 cm^{-1}, respectively.[18] Similar results are obtained theoretically at the MRCI+Q/5Z level, that is, T_e = 3127 [A $^1\Delta(1)$] and 3155 [b $^3\Pi(1)$] cm^{-1}. Bond distances are predicted fairly well taking into account core effects ($3s^23p^6$) at the C-MRCI+Q/C4Z level, namely r_e(A $^1\Delta$) = 2.383 Å (MRCI+Q/5Z) − 0.037 = 2.346 Å and r_e(b $^3\Pi$) = 2.395 Å (MRCI+Q/5Z) − 0.031 = 2.364 Å; corresponding experimental values are 2.339 and 2.344 Å[18] (Table 3). Dipole moments of 2.6 and 3.6 D are recommended for the A $^1\Delta(1)$ and b $^3\Pi(1)$ states.

Experimentally, the next two pairs of states c $^3\Sigma^+(1)$ and B $^1\Pi(1)$ are located 5385 and 6020.5 cm^{-1} above the X $^1\Sigma^+$ state, in very good agreement with the calculated MRCI+Q/5Z values 5071 and 6049 cm^{-1}, respectively. Bond distances corrected for core effects at the C-MRCI+Q/C4Z level are r_e[c $^3\Sigma^+(1)$] = 2.395 (MRCI+Q/5Z) −0.029 = 2.366 Å and r_e[B $^1\Pi(1)$] = 2.405 (MRCI+Q/5Z) − 0.027 = 2.378 Å, 0.02 and 0.03 Å longer than the experimental ones.[18] Recommended dipole moments are 2.5 [c $^3\Sigma^+(1)$] and 4.4 [B $^1\Pi(1)$] D.

The energy level diagram of Figure 3 compares the loci of experimentally determined excited states of ScCl within an energy range of ∼3.0 eV, with theoretical results of the present work at the MRCI+Q/5Z [X $^1\Sigma^+$, a $^3\Delta(1)$, A $^1\Delta(1)$, b $^3\Pi(1)$, c $^3\Sigma^+(1)$, B $^1\Pi(1)$], and MRCI+Q/4Z (rest of the states) level. Observe the relative good agreement in the energy separations between theory and experiment.

It is useful at this point to recall that the first six states of ScF, isovalent to ScCl, correlate diabatically to the ^{3}D($4s^13d^1$)

and $^1D(4s^13d^1)$ terms of Sc^+ and follow the same state ordering. Specifically, the experimental T_{00} (cm^{-1}) and r_0 (Å) values of ScF are 0.0, 1969.0,[28] 4542.235,[30] 6285.003,[28] 9413.276,[31] 9441.702[31] and 1.7873(r_e),[32] 1.8598,[28] 1.8632,[30] 1.8911,[28] 1.9130,[31] 1.9090[31] for the states X $^1\Sigma^+$, a $^3\Delta$, A $^1\Delta$, b $^3\Pi$, c $^3\Sigma^+$, B $^1\Pi$, respectively, in complete analogy with the corresponding states of ScCl, in both the ordering of states and the trend in bond lengths.

B. States d $^3\Delta(2)$, e $^3\Phi(1)$, C $^1\Sigma^+(2)$, $^3\Pi(2)$, $^3\Sigma^-(1)$, $^3\Pi(3)$, D $^1\Pi(2)$, $^1\Delta(2)$, $^3\Sigma^-(2)$, $^3\Phi(2)$, and $^3\Pi(4)$. The 11 states above crowded in an energy range of about 1.4 eV have been examined at the MRCI+Q/4Z level; for three states, that is, d $^3\Delta(2)$, e $^3\Phi(1)$, and C $^1\Sigma^+(2)$ C-MRCI/C4Z, calculations have also been performed. Potential energy curves are displayed in Figure 2, whereas experimental and theoretical energy levels are contrasted in Figure 3; numerical results are compiled in Table 3. Because of the very complex nature of these states, we limit our discussion to some general remarks.

All states are of multireference character, ionic, with a charge transfer of about 0.7 e^- from Sc to Cl(^2P; M_L=0), and considerably bound even with respect to the ground-state atoms Sc(^2D) + Cl(^2P). For instance, the highest of these states, $^3\Pi(4)$, has a MRCI(+Q)/4Z D_e = 26.5 (32.1) kcal/mol with respect to the ground-state atoms. With the exception of e $^3\Phi(1)$, d $^3\Delta(2)$, and $^3\Phi(2)$ where we can infer with certainty their adiabatic fragments, i.e., Sc($^4F;4s^13d^2$) and c($^4F^0;3d^14s^14p^1$) respectively, MRCI(+Q)/4Z D_e adiabatic values are also determined for the $3\Sigma^-(1)$, $^3\Pi(2)$, $^3\Pi(3)$, and $^3\Pi(4)$ states but not without some reservations due to the complexity of their PECs; see Figure 2. For the remaining four states, C $^1\Sigma^+(2)$, D $^1\Pi(2)$, $^1\Delta(2)$, and $^3\Sigma^-(2)$ no D_e values are given in Table 3, the reason being the uncertainty of their end terms.

From Figure 3 we note that the $^3\Pi(2)$, $^3\Sigma^-(1)$, and $^3\Sigma^-(2)$ states located 15413 (15122), 15267 (15253), and 21513 (20689) cm^{-1} above the X-state and within the experimental energy range examined, have not been observed experimentally. The calculated states $^3\Phi(2)$ and $^3\Pi(4)$ with T_e = 25382 (24837) and 25762 (25067) cm^{-1} are out of the experimentally probed energy span. Finally, most of the states studied here are characterized by large to very large dipole moments; in particular μ_{FF} values around 7−8 D are computed for the highest three states $^3\Sigma^-(2)$, $^3\Phi(2)$, and $^3\Pi(4)$, close to their "classical" value obtained by a charge transfer of about 0.7 e^- and a bond distance of 2.4 Å; see Table 3.

5. Results and Discussion on TiCl

Experimental and ab initio theoretical results from the literature on TiCl are given in Table 4; a density functional theory (DFT) work has also been published in 1998.[41] Experimentally, the states X $^4\Phi$, C $^4\Delta$, a ^2F, and G $^4\Phi$ have been investigated through spectroscopic methods.[34−37] In addition Ram and Bernath via infrared emission spectroscopy in the 4200−8500 cm^{-1} range observed a $^2\Sigma^-$−$^2\Sigma^-$ or $^2\Sigma^+$−$^2\Sigma^+$ transition, the energy separation between the two Σ states being T_{00} = 6938.864 89(37) cm^{-1}.[42] Finally, a $^4\Gamma$ state has been observed by high-resolution Fourier transform emission spectroscopy located close to T_{00} = 24 000 cm^{-1}, the exact value depending on the $|\Omega| = |\Lambda+\Sigma|$ coupling of both X $^4\Phi$ and $^4\Gamma$ states.[43]

Ab initio theoretical works on TiCl are limited to X $^4\Phi$, $^4\Sigma^-$, and $^2\Delta$ states;[38−40] see Table 4. The most thorough study is that of Bauschlicher through the CCSD(T) method in conjunction with correlation consistent basis sets of his own.[39] In particular, by using a series of triple (T), quadruple (Q), and quintuple (5) cardinality bases, he obtained for the X $^4\Phi$ state only a complete basis set (CBS) limit value for the dissociation energy, D_0 = 98.7 kcal/mol. In obtaining this value, core-correlation effects of Ti($3s^23p^6$) and DKH scalar relativistic effects calculated at the modified coupled-pair functional MCPF/(valence)TZ level + semiempirical corrections for spin−orbit coupling have been taken into account. The bond distance and harmonic frequency, r_e = 2.274 Å and ω_e = 400 cm^{-1}, have been calculated at the C-CCSD(T)/C5Z level with no further corrections.[39]

TABLE 4: Existing Experimental and Theoretical Data on $Ti^{35}Cl$. Dissociation Energies D_0 (kcal/mol), Bond Distances r_e (Å), Harmonic Frequencies ω_e (cm^{-1}), Rotational−Vibrational Constants α_e (cm^{-1}), and Energy Separations T_e (cm^{-1})

state	D_0	r_e	ω_e	$\alpha_e \times 10^3$	T_e
		Experimental Results			
X $^4\Phi$	101.3[a]	2.2647[b]	404.33[b,c]	0.80[b]	0.0
X $^4\Phi$[d]		2.26462345(15)		0.8042	0.0
C $^4\Delta$		2.2972379(68)[d,e]	366 ± 7[f,c]		3281.71[b,g]
G $^4\Phi$[b]		2.3494[e]			10904.04
a $^2\Phi_{7/2}$[h]		2.19031(75)	423.9036(27)	1.03(8)	
		Ab Initio Results			
X $^4\Phi$[i]	90.6	2.311	393		0.0
X $^4\Phi$[j]	98.7	2.274	400		0.0
X $^4\Phi$[k]		2.319	382	0.72	0.0
$^4\Sigma^{-1}$		2.288	398		1903
$^4\Sigma^{-k}$		2.318	374	0.72	1024
$^2\Delta$[m]		2.336			2807
$^2\Delta$[k]		2.257	377	0.81	3347

[a] Reference 33a, thermochemistry. [b] Reference 34, Fourier transform infrared (FTIR) spectroscopy. [c] $\Delta G_{1/2}$ ($\approx\omega_e - 2\omega_e x_e$). [d] Reference 35, submillimeter-wave spectroscopy. [e] r_0 value. [f] Reference 36, high-resolution laser spectroscopy. [g] T_{00} value. [h] Reference 37; $\omega_e x_e$ = 0.4226(12) cm^{-1}. An r_e = 2.19565(10) Å is also reported for a $^2\Phi_{5/2}$ state. FTIR spectroscopy. [i] Reference 38; valence-CCSD(T)/6-311++G(2d, 2f), E = −1308.199406 E_h,μ_e[QCISD/6-311++G(d, f)] = 3.863 D. [j] Reference 39; r_e and ω_e obtained at the C-CCSD(T)/C5Z level. See text for details. [k] Reference 40; MRCI+Q/ model core potential for the first 12 inner electrons of Ti. [l] Reference 38; see footnote (i). μ_e = 3.868 D. [m] Reference 38; see footnote (i). μ_e = 3.168 D.

Considering the TiCl species as ionic enough, indeed about 0.6−0.7 e^- are transferred from Ti to Cl according to the MRCI Mulliken distributions, the $\Lambda-\Sigma$ low-lying molecular states can be deduced as usual from Ti^+ in the field of $Cl^-(^1S)$. The ground term of Ti^+ is $^4F(4s^13d^2)$ with the $^4F(3d^3)$ and $^2F(4s^13d^2)$ terms located 860.27 and 4557.16 cm^{-1} (M_J averaged) higher.[16] In the field of Cl^-, the first two quartets give rise to eight quartets of Σ, Π, Δ, and Φ symmetry, while four doublets of the same spatial symmetry stem from the ^2F term. On the other hand, the neutral atoms, Ti(^3F; $4s^23d^2$) + Cl(^2P), give rise to 24 molecular states doublets and quartets, i.e., $^{2,4}[\Sigma^{\pm}, \Sigma^-, \Pi(3), \Delta(3), \Phi(2), \Gamma]$. We have calculated the PECs of four quartets (X $^4\Phi$, A $^4\Sigma^-$, B $^4\Pi$, C $^2\Delta$) followed by four doublets (a $^2\Delta$, b $^2\Phi$, c $^2\Pi$, d $^2\Sigma^-$), all correlating adiabatically to the neutral ground-state atoms Ti(^3F) + Cl(^2P); see Figure 4. Observe that the sheaf of the four quartets suffer an avoided crossing with their ionic diabatic companions $Ti^+(4s^13d^2) + Cl^-$ at 5.2 Å; the analogous avoided crossing of the four doublets occur at 4.6 Å and are related to the diabatic fragments $Ti^+(^2F;4s^13d^2) + Cl^-(^1S)$. The MRCI(+$Q$)/4Z X $^4\Phi$−b $^2\Phi$ (or a $^2\Delta$) splitting is calculated to be 4400 (4202) cm^{-1}, reflecting the atomic $^4F(4s^13d^2)$−^2F Ti^+ energy difference of 4557 cm^{-1}.

Table 5 lists numerical results; as in ScCl the first two states X $^4\Phi$ and A $^4\Sigma^-$ have been examined much more thoroughly than the rest of the states for which our calculations have been

limited to the MRCI(+*Q*)/4Z and C-MRCI(+*Q*)/C4Z levels of theory. We discuss first the quartets followed by the doublets.

A. States X $^4\Phi$, A $^4\Sigma^-$, B $^4\Pi$, and C $^4\Delta$. Following the notation introduced previously in ScCl, that is, suppressing the 28 core electrons, the leading equilibrium MRCI/4Z configurations and Mulliken atomic populations are

$$|X^4\Phi\rangle_{B_1} = {}^1/_{\sqrt{2}}|1\sigma^2 2\sigma^2 3\sigma^1 1\pi_x^2 1\pi_y^2(2\pi_x^1 1\delta_+^1 + 2\pi_y^1 1\delta_-^1)\rangle$$

$$4s^{0.85}4p_z^{0.23}4p_{x,y}^{0.06}3d_{z^2}^{0.14}3d_{xz}^{0.53}3d_{yz}^{0.53}3d_{x^2-y^2}^{0.50}3d_{xy}^{0.50}/Cl^{\delta-},\delta = 0.63$$

Dropping further the part $1\sigma^2 2\sigma^2 1\pi_x^2 1\pi_y^2 (\sim 3s^2 3p_z^2 3p_x^2 3p_y^2$ of Cl^-) common to all MCls (M = Sc−Cr), we write

$$|X^4\Phi\rangle_{B_1} = {}^1/_{\sqrt{2}}|3\sigma^1(2\pi_x^1 1\delta_+^1 + 2\pi_y^1 1\delta_-^1)\rangle$$

counting only the Ti^+ "valence" electrons. Following this very compact notation from now on, we have

$$|A^4\Sigma^-\rangle_{A_2} \approx |0.70(3\sigma^1 2\pi_x^1 2\pi_y^1) - 0.65(3\sigma^1 1\delta_+^1 1\delta_-^1)\rangle$$

$$4s^{0.86}4p_z^{0.24}4p_{x,y}^{0.06}3d_{z^2}^{0.13}3d_{xz}^{0.56}3d_{yz}^{0.56}3d_{x^2-y^2}^{0.46}3d_{xy}^{0.46}/Cl^{\delta-},\delta = 0.63$$

$$|B^4\Pi\rangle_{B_1} \approx |0.60[(3\sigma^1 2\pi_y^1 1\delta_-^1) - (3\sigma^1 2\pi_x^1 1\delta_+^1)] - 0.43(3\sigma^1 4\sigma^1 2\pi_x^1)\rangle$$

$$4s^{0.85}4p_z^{0.25}4p_{x,y}^{0.06}3d_{z^2}^{0.31}3d_{xz}^{0.63}3d_{yz}^{0.43}3d_{x^2-y^2}^{0.39}3d_{xy}^{0.40}/Cl^{\delta-},\delta = 0.64$$

$$|C^4\Delta\rangle_{A_2} \approx 0.96|3\sigma^1 4\sigma^1 1\delta_-^1\rangle$$

$$4s^{0.87}4p_z^{0.32}4p_{x,y}^{0.04}3d_{z^2}^{1.0}3d_{xz}^{0.05}3d_{yz}^{0.05}3d_{xy}^{1.0}/Cl^{\delta-},\delta = 0.64$$

Note that the configurations given represent the cation Ti^+ and that, consistently, about 0.65 e^- are transferred from Ti to Cl at equilibrium. The configurations above and their populations are remarkably similar to those of the corresponding TiF quartets following as well the same order.[3]

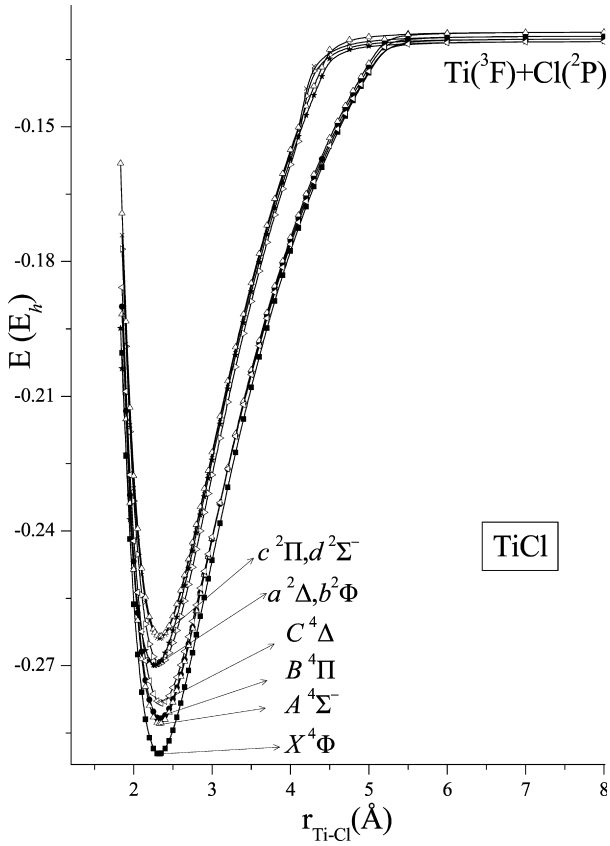

Figure 4. MRCI/4Z potential energy curves of the TiCl molecule. Energies are shifted by +1308 E_h.

As can be seen from Table 5 at the C-MRCI(+*Q*)/C5Z level, D_e = 100.6 (102.1) kcal/mol. The contribution of scalar relativistic effects, either valence (4Z) or core (C4Z), is persistently negative, −1.4 (−1.5) kcal/mol, therefore D_e = 100.6 (102.1) −1.4 (−1.5) = 99.2 (100.6) kcal/mol, or $D_0 = D_e - \omega_e/2$ = 99.2 (100.6) −0.6 = 98.6 (100.0) kcal/mol with respect to Ti (^{4}F) + Cl(^{2}P). At the highest CC level C-RCCSD(T)+DKH2/C5Z, we obtain D_e (D_0) = 97.8 (97.2) kcal/mol. Taking the mean value of MRCI and CC methods, we suggest D_0 = 98.5 ± 1.5 kcal/mol, in good agreement with the experimental thermochemical value D_0^o = 101.3 ± 2 kcal/mol.[33a]

At the MRCI level the bond length of the X $^4\Phi$ state converges to r_e[C-MRCI(+*Q*)/C5Z] = 2.300 (2.286) Å, with negligible contribution from scalar relativity. Core effects of the metal are responsible for a shortening of 0.02 Å in both C4Z and C5Z basis sets. The 2.286 Å distance is 0.02 Å larger than the experimental value; see Table 5. The CC r_e converges to 2.276 Å [C-RCCSD(T)+DKH2/C5Z]; including a 0.003 Å reduction due to the core electrons of Cl ($2s^2 2p^6$) obtained at the C^2-RCCSD(T)/$C^2$4Z level, we finally obtain r_e = 2.273 Å, 0.008 Å longer than the experimental one.[35]

The experimental value of $\Delta G_{1/2}$ is $\Delta G_{1/2}(\approx \omega_e - 2\omega_e x_e)$ = 404.33;[34] using an $\omega_e x_e$ = 1.4 cm^{-1} (Table 5), ω_e = 404.33 + 2.8 = 407 cm^{-1}, in perfect agreement with our best CC value. Finally, by both MRCI and CC methods the dipole moment obtained by the finite field approach is very close to μ_e = 3.8 D. Note the difference $\langle\mu\rangle - \mu_{FF} \approx 0.3$ D at the MRCI level.[27]

The first excited state of TiCl, A $^4\Sigma^-$, has not been observed experimentally ($\Delta\Lambda = \pm 3$); existing ab initio results on A $^4\Sigma^-$ are presented in Table 4.

As can be seen from Table 5 the influence of the $3s^2 3p^6$ electrons of the metal in the energy distance T_e(A $^4\Sigma^-$−X $^4\Phi$) is about 10% at the MRCI/4Z vs C-MRCI/C4Z level, whereas the effect of scalar relativity is practically none. At the highest multireference level, C-MRCI(+*Q*)/C5Z, we get T_e = 1323 (1251) cm^{-1} at r_e = 2.309 (2.293) Å. On the other hand, the CC-numbers look problematic: The T_e separation is doubled in both the quadruple and quintuple basis sets as we move from the valence to the core level, 1695 vs 3363 cm^{-1} and 1709 vs 3373 cm^{-1}, respectively. Including relativistic effects (C-RCCSD(T)+DKH2/C5Z) give T_e = 3329 cm^{-1}, practically negligible contribution in conformity with the MRCI results. The multireference character of the A $^4\Sigma^-$ state (vide supra) seems to be the cause of the problem; therefore, we disregard the CC-numbers for the A $^4\Sigma^-$ state. It is worthwhile to note, however, that r_e and μ_e values of A $^4\Sigma^-$ are in accordance in both MRCI and CC methods, indicating again the complexity of these systems.

As a final conclusion for the A $^4\Sigma^-$ state, we can claim with enough confidence that the A $^4\Sigma^-$−X $^4\Phi$ splitting is not larger than 1500 cm^{-1} (=4.3 kcal/mol), r_e = 2.290 Å (taking into account the core effect of Cl), and μ_{FF} = 3.7 D.

The next quartet, B $^4\Pi$, is practically degenerate with the A $^4\Sigma^-$ state at least at the level of our calculations. According to Table 5, ΔE(B $^4\Pi$−A $^4\Sigma^-$) = 239 (227) and 409 (419) cm^{-1} at MRCI(+*Q*)/4Z and C-MRCI(+*Q*)/C4Z, respectively. The corresponding splitting in TiF and at the same level of theory is close to 1500 cm^{-1},[3] whereas the recommended dipole moment is μ_{FF} = 3.7 D.

The last calculated quartet, C $^4\Delta$, is of single reference character (vide supra) and relatively well separated from the

TABLE 5: Total Energies E (E_h), Dissociation Energies D_e (kcal/mol), Bond Distances r_e (Å), Harmonic and Anharmonic Frequencies ω_e, $\omega_e x_e$ (cm^{-1}), Rotational−Vibrational Constants α_e (cm^{-1}), Centrifugal Distortions $\bar{D}_e$ (cm^{-1}), Dipole Moments μ_e (D), and Energy Separations T_e (cm^{-1}) of $^{48}Ti^{35}Cl$

method/basis set[a]	$-E$	D_e	r_e	ω_e	$\omega_e x_e$	$\alpha_e \times 10^3$	$\bar{D}_e \times 10^7$	$\langle\mu\rangle$ (μ_{FF})[b]	T_e
			X $^4\Phi$						
MRCI/4Z	1308.289592	99.9	2.321	389	1.35	0.766	0.981	3.36 (3.76)	0.0
MRCI+*Q*	1308.312776	100.1	2.312	390	1.35	0.770	0.995		0.0
C-MRCI/C4Z	1308.610847	99.8	2.303	395	1.38	0.778	0.994	3.30 (3.81)	0.0
C-MRCI+*Q*	1308.679395	101.1	2.288	399	1.38	0.784	1.013		0.0
MRCI+DKH2/4Z	1313.032323	98.5	2.320	389	1.35	0.770	0.986	3.37 (3.76)	0.0
MRCI+DKH2+*Q*	1313.055499	98.7	2.311	390	1.36	0.774	1.000		0.0
C-MRCI+DKH2/C4Z	1313.353534	98.4	2.302	396				3.30 (3.76)	0.0
C-MRCI+DKH2+*Q*	1313.421930	99.6	2.288	389					0.0
MRCI/5Z	1308.296595	100.7	2.319	389				3.34 (3.73)	0.0
MRCI+*Q*	1308.320344	101.0	2.309	384					0.0
C-MRCI/C5Z	1308.623125	100.6	2.300	397				3.27 (3.83)	0.0
C-MRCI+*Q*	1308.692785	102.1	2.286	389					0.0
RCCSD(T)/4Z	1308.316130	99.7	2.312	388	1.35	0.778	1.006	... (3.66)	0.0
C-RCCSD(T)/C4Z	1308.696715	102.4	2.280	399	1.37	0.804	0.967	... (3.76)	0.0
C^2-RCCSD(T)/C^2QZ	1309.035687	102.7	2.277	400	1.41	0.812	1.040	... (3.76)	0.0
RCCSD(T)+DKH2/4Z	1314.058955	96.2	2.311	393				... (3.67)	0.0
C-RCCSD(T)+DKH2/C4Z	1314.439368	96.6	2.279	402				... (3.60)	0.0
RCCSD(T)/5Z	1308.324326	99.1	2.310	389				... (3.64)	0.0
C-RCCSD(T)/C5Z	1308.711415	99.8	2.277	399				... (3.83)	0.0
C-RCCSD(T)+DKH2/C5Z	1314.454251	97.8	2.276	407				... (3.71)	0.0
expt		101.3[c]	2.26462345(15)[d]	404.33[e]		0.8042[d]			
			A $^4\Sigma^-$						
MRCI/4Z	1308.282911	96.7	2.329	383	1.33	0.770	0.992	3.18 (3.71)	1466
MRCI+*Q*	1308.306268	96.7	2.319	384	1.33	0.775	1.010		1428
C-MRCI/C4Z	1308.604796	96.5	2.311	389	1.36	0.783	1.006	3.06 (3.76)	1328
C-MRCI+*Q*	1308.673643	97.7	2.296	392	1.36	0.790	1.029		1262
MRCI+DKH2/4Z	1313.025729	95.3	2.327	383	1.33	0.778	0.991	3.20 (3.71)	1447
MRCI+DKH2+*Q*	1313.049111	95.3	2.317	384	1.25	0.804	1.000		1402
C-MRCI+DKH2/C4Z	1314.347590	94.6	2.310	388				3.08 (3.78)	1305
C-MRCI+DKH2+*Q*	1314.416334	96.1	2.294	380					1228
MRCI/5Z	1308.289901	97.5	2.327	382				3.16 (3.70)	1469
MRCI+*Q*	1308.313836	97.6	2.316	376					1428
C-MRCI/C5Z	1308.617098	97.3	2.309	389				3.03 (3.77)	1323
C-MRCI+Q	1308.687084	98.7	2.293	381					1251
RCCSD(T)/4Z	1308.308407	94.8	2.334	381	1.29	0.765	0.988	... (3.76)	1695
C-RCCSD(T)/C4Z	1308.681393	92.8	2.309	387	1.41	0.787	1.021	... (3.91)	3363
C^2-RCCSD(T)/$C^2$4Z	1309.020345	93.1	2.306	387	1.43	0.805	1.028	... (3.87)	3367
C-RCCSD(T)+DKH2/C4Z	1314.424198	87.1	2.308	391				... (3.86)	3329
RCCSD(T)/5Z	1308.316541	94.2	2.331	386				... (3.75)	1709
C-RCCSD(T)/C5Z	1308.696046	90.1	2.305	386				... (3.92)	3373
			B $^4\Pi$						
MRCI/4Z	1308.281821	95.4	2.335	379	1.33	0.772	0.996	3.30 (3.56)	1705
MRCI+*Q*	1308.305237	95.5	2.324	381	1.34	0.777	1.012		1655
C-MRCI/C4Z	1308.602932	95.1	2.317	385	1.36	0.784	1.011	3.26 (3.66)	1737
C-MRCI+*Q*	1308.671736	96.4	2.301	389	1.37	0.792	1.033		1681
			C $^4\Delta$						
MRCI/4Z	1308.278353	92.5	2.349	366	1.25	0.759	1.028	2.66 (2.64)	2467
MRCI+*Q*	1308.301581	92.7	2.339	368	1.24	0.766	1.045		2457
C-MRCI/C4Z	1308.598150	91.6	2.333	371	1.28	0.771	1.042	2.69 (2.64)	2787
C-MRCI+*Q*	1308.666500	92.8	2.318	375	1.28	0.781	1.064		2830
C-MRCI/C5Z	1308.610357	93.1	2.331	388				2.65 (2.64)	2802
C-MRCI+*Q*	1308.679820	94.1	2.315	380					2845
RCCSD(T)/4Z	1308.306867	92.4	2.338	368	1.22	0.766	1.049	... (2.41)	2033
C-RCCSD(T)/C4Z	1308.685893	92.0	2.310	377				... (2.26)	2375
expt			2.2972379(68)[d,f]	366 ± 7[g]					3281.71[h]
			a $^2\Delta$						
MRCI/4Z	1308.269953	87.2	2.271	379	1.18	0.845	1.177	2.61 (3.15)	4310
MRCI+*Q*	1308.296754	89.7	2.246	386	1.22	0.911	1.210		3516
C-MRCI/C4Z	1308.588122	85.3	2.256	385	1.23	0.848	1.184	2.55 (3.25)	4988
C-MRCI+*Q*	1308.660312	88.9	2.225	395	1.24	0.921	1.220		4188
			b $^2\Phi$						
MRCI/4Z	1308.269545	87.3	2.332	388	1.34	0.761	0.956	2.90 (3.25)	4400
MRCI+*Q*	1308.293630	88.0	2.324	389	1.35	0.765	0.970		4202
C-MRCI/C4Z	1308.588762	85.9	2.314	395	1.37	0.771	0.969	2.79 (3.25)	4847

TABLE 5: Continued

method/basis set[a]	$-E$	D_e	r_e	ω_e	$\omega_e x_e$	$\alpha_e \times 10^3$	$\bar{D}_e \times 10^7$	$\langle\mu\rangle$ (μ_{FF})[b]	T_e
C-MRCI+Q	1308.657888	87.6	2.301	398	1.37	0.778	0.988		4720
expt[i]			2.19031(75)	423.9036(27)	1.03(8)				
				c $^2\Pi$					
MRCI/4Z	1308.263932	84.2	2.329	381	1.34	0.758	1.003	3.01 (3.51)	5632
MRCI+Q	1308.288845	85.2	2.317	382	1.35	0.760	1.028		5252
C-MRCI/C4Z	1308.582994	82.6	2.312	387	1.37	0.769	1.012	2.90 (3.51)	6113
C-MRCI+Q	1308.653034	84.7	2.295	390	1.37	0.771	1.042		5786
				d $^2\Sigma^-$					
MRCI/4Z	1308.263462	84.5	2.333	383	1.34	0.769	0.977	2.84 (3.15)	5735
MRCI+Q	1308.287763	85.1	2.324	384	1.32	0.773	0.994		5490
C-MRCI/C4Z	1308.583712	83.3	2.313	391	1.36	0.783	0.992	2.72 (3.10)	5955
C-MRCI+Q	1308.653373	85.0	2.299	393	1.36	0.792	1.013		5711

[a] +Q refers to the Davidson correction; C- and C^2- means that the $3s^23p^6$ and $2s^22p^6$ electrons of Ti and Cl, respectively, have been included in the CI. [b] $\langle\mu\rangle$ calculated as an expectation value, μ_{FF} by the finite field approach; field strength 5×10^{-5} au. [c] D_0 value, ref 33a. [d] Reference 35. [e] Reference 34, $\Delta G_{1/2}$ value. [f] r_0 value. [g] Reference 36, $\Delta G_{1/2}$ value. [h] T_{00} value, ref 34. [i] Reference 37, but see text.

A $^4\Sigma^-$, B $^4\Pi$ pair. Concerning r_e, the MRCI results converge monotonically to 2.315 Å whereas the C-RCCSD(T)/C4Z predicts $r_e = 2.310$ Å in relatively good agreement with experiment.[35] Judging from our previous results, it is certain that increasing the basis set to C5Z and including the core effects of Cl($2s^22p^6$), the r_e CC value will be reduced by at least 0.005 Å, that is $r_e = 2.310-0.005 = 2.305$ Å, now in very good agreement with the experimental r_0 value of 2.2972 Å; see Table 5. Our best MRCI+Q T_e(C $^4\Delta-$X $^4\Phi$) separation is 2845 cm^{-1} as contrasted to $T_{00} = 3282$ cm^{-1} of the experiment. Finally, trusting more the CC dipole moment, a $\mu_e = 2.3$ D is suggested.

B. States a $^2\Delta$, b $^2\Phi$, c $^2\Pi$, and d $^2\Sigma^-$. Following the notation introduced in section 5A the leading equilibrium configurations ($|Ti^+\rangle$) of the doublets along with their Mulliken populations are

$$|a^2\Delta\rangle_{A_2} \approx 0.70|3\sigma^2 1\delta_-^1\rangle + 0.41|3\sigma^1 4\sigma^1 1\bar{\delta}_-^1\rangle + 0.36|3\sigma^1 4\bar{\sigma}^1 1\delta_-^1\rangle + 0.33|4\sigma^2 1\delta_-^1\rangle$$

$$4s^{1.04}4p_z^{0.24}4p_{x,y}^{0.06}3d_{z^2}^{0.94}3d_{xz}^{0.06}3d_{yz}^{0.06}3d_{xy}^{0.99}/Cl^{\delta-}, \delta = 0.57$$

$$|b^2\Phi\rangle_{B_1} \approx 0.58|3\sigma^1 2\pi_x^1 1\bar{\delta}_+^1\rangle - 0.58|3\sigma^1 2\bar{\pi}_y^1 1\delta_-^1\rangle - 0.34|3\sigma^1 2\pi_y^1 1\bar{\delta}_-^1\rangle + 0.33|3\sigma^1 2\bar{\pi}_x^1 1\delta_+^1\rangle$$

$$4s^{0.87}4p_z^{0.26}4p_{x,y}^{0.06}3d_{z^2}^{0.14}3d_{xz}^{0.54}3d_{yz}^{0.54}3d_{x^2-y^2}^{0.50}3d_{xy}^{0.50}/Cl^{\delta-}, \delta = 0.58$$

$$|c^2\Pi\rangle_{B_1} \approx 0.51|3\sigma^1 2\pi_x^1 1\bar{\delta}_+^1\rangle + 0.49|3\sigma^1 2\bar{\pi}_y^1 1\delta_-^1\rangle + 0.40|3\sigma^1 4\bar{\sigma}^1 2\pi_x^1\rangle + 0.31|3\sigma^1 2\pi_y^1 1\bar{\delta}_-^1\rangle + 0.31|3\sigma^1 2\pi_y^1 1\bar{\delta}_-^1\rangle + 0.26|3\sigma^1 2\bar{\pi}_x^1 1\delta_+^1\rangle$$

$$4s^{0.90}4p_z^{0.25}4p_{x,y}^{0.05}3d_{z^2}^{0.34}3d_{xz}^{0.66}3d_{yz}^{0.41}3d_{x^2-y^2}^{0.37}3d_{xy}^{0.37}/Cl^{\delta-}, \delta = 0.63$$

$$|d^2\Sigma^-\rangle_{A_2} \approx 0.54|3\sigma^1 2\bar{\pi}_x^1 2\pi_y^1\rangle - 0.53|3\sigma^1 1\delta_+^1 1\delta_-^1\rangle + 0.31|3\sigma^1 2\pi_x^1 2\bar{\pi}_y^1\rangle + 0.31|3\sigma^1 1\delta_+^1 1\bar{\delta}_-^1\rangle + 0.25|4\bar{\sigma}^1 1\delta_+^1 1\delta_-^1\rangle - 0.20|4\sigma^1 2\bar{\pi}_x^1 2\pi_y^1\rangle$$

$$4s^{0.86}4p_z^{0.26}4p_{x,y}^{0.06}3d_{z^2}^{0.13}3d_{xz}^{0.51}3d_{yz}^{0.51}3d_{x^2-y^2}^{0.53}3d_{xy}^{0.53}/Cl^{\delta-}, \delta = 0.62$$

Notice the intense multireference character of the doublets and that about 0.6 e$^-$ are transferred from Ti to Cl. We remind that only the $^2\Phi_{7/2}$ and $^2\Phi_{5/2}$ have been observed experimentally by FTIR spectroscopy (Table 4). However, some reservations have been expressed by the experimentalists on the identity of the $^2\Phi$ state;[37] in verbatim: "At this stage we are unable to confirm definitely whether the observed lowest doublet state is a $^2\Delta$ or $^2\Phi$ state but the absence of Ω doubling in the observed bands indicates that the doublet states of Ω>1 are involved in this transition of TiCl and ZrCl. In this paper we have preferred to label the lower state as the $^2\Phi$ state. It is possible, but less likely, that our bands belong to a $^2\Delta-^2\Delta$ transition. Note that the assignment of the 7/2 and 5/2 spin components was based only on the relative size of the effective B values in the $^2\Phi$ state and is also not secure."

The $^2\Delta$ and $^2\Phi$ states have been formally tagged as a $^2\Delta$ and b $^2\Phi$ according to our MRCI results. We cannot be sure, however, of this ordering considering the pitfalls of the MRCI approach, the C-MRCI+Q/C4Z ΔE ($^2\Delta-^2\Phi$) being 141 (532) cm^{-1}; we can only say that the $^2\Delta$ and $^2\Phi$ states are very close in energy. On the other hand, based on the bond distance $r_e = 2.225$ Å of the a $^2\Delta$ state, which is certainly shorter by at least 0.005 Å (vide supra), the state assigned to $^2\Phi$ by Ram and Bernath[37] could very well be a $^2\Delta$ state as also suggested by these authors. Obviously, very high level calculations are needed to resolve this question. Dipole moments for both states based on the finite field method are close to 3.2 D.

The next two doublets, formally named as c $^2\Pi$ and d $^2\Sigma^-$, are also degenerate within the accuracy of our calculations (Table 5 and Figure 4), but relatively well separated from the (a $^2\Delta$, b $^2\Phi$) pair, located about 6000 cm^{-1} above the X-state and with similar bond distances $r_e \approx 2.30$ Å. Recommended dipole moments are 3.50 (c $^2\Pi$) and 3.1 (d $^2\Sigma^-$) D.

6. Results and Discussion on VCl

Very little is known experimentally on the VCl radical; as far as we know, the experimental literature on VCl is exhausted in four publications. It seems that the emission spectrum of VCl was observed for the first time in 1970 by Iacocca et al.[44] More than 30 years later its high-resolution FTIR emission spectrum was recorded in the 3000−9400 cm^{-1} region by Ram et al.[45] Through the rotational analysis of the 0−1 and 0−0 vibrational bands of the [7.0] $^5\Delta-$X $^5\Delta$ emission, these workers obtained molecular constants of the X $^5\Delta$ state, namely, $r_e = 2.213\,79(170)$ Å, $\Delta G_{1/2} = 415.26(113)$ cm^{-1}, and $\alpha_e = 0.000\,856(84)$ cm^{-1}. It is also of interest what is stated in ref 45: "Most likely the lower X $^5\Delta$ state is the ground state but we do not have any direct evidence to prove this." Two years later, Ram et al.[46] examined the FTIR spectrum of VCl in the 3000−19400 cm^{-1} region, and with the help of ab initio calculations (see below) the previously assigned [7.0] $^5\Delta-$X $^5\Delta$ transition[45] was reassigned to E $^5\Delta-$X $^5\Delta$. For the X $^5\Delta$ state they redetermined

the bond length, $r_e = 2.2145$ Å, and two more parameters, $\omega_e = 417.4$ cm^{-1} and $\omega_e x_e = 3.5$ cm^{-1}. In addition, for the E $^5\Delta$ state (but see below) the following molecular parameters have been obtained, $r_e = 2.2952$ Å, $\Delta G_{1/2} = 354.1$ cm^{-1}, $\alpha_e = 0.0009$ cm^{-1}, and T_0(E $^5\Delta$−X $^5\Delta$) = 7001.928 cm^{-1}.

In the last thermochemical experimental work on VCl, the dissociation energy was determined to be $D_0^o = 101.9 \pm 2$ kcal/mol.[47]

The only theoretical work on VCl is that of Ram et al.[46] who performed (valence) MRCI+Q state averaged calculations, employing 10-core electron relativistic pseudopotentials for both atoms + valence basis sets ([6s5p3d1f/$_V$ 4s4p/$_{Cl}$]) of the Stuttgart group.[48] They calculated 11 states around equilibrium, four triplets, and seven quintets, determining r_e, ω_e, and T_{00} and dipole moments for four quintets. Their findings are compared with the results of the present work in Table 6.

Considering that at equilibrium more than 0.6 e$^-$ are transferred to the Cl atom (vide infra), the ensuing Λ−Σ states of VCl can be related to the V^+ terms in the field of Cl^-(^{1}S). The first three terms of V^+ are ^{5}D(3d^4), ^{5}F(4s^{1}3d^3), and ^{3}F(4s^{1}3d^3), the last two located 2719.89 and 8697.32 cm^{-1} (M_J-averaged) above the ^{5}D.[16] The lifting of the M_L degeneracy of these terms in the field of Cl^- gives rise to 11 $^{2S+1}|\Lambda|$ V^+Cl^- states, triplets, and quintets: ($^5\Sigma^+$, $^5\Pi$, $^5\Delta$), ($^5\Sigma^-$, $^5\Pi$, $^5\Delta$, $^5\Phi$), and ($^3\Sigma^-$, $^3\Pi$, $^3\Delta$, $^3\Phi$) related to ^{5}D, ^{5}F, and ^{3}F atomic states of V^+, respectively. We have constructed complete PECs of all these states at the MRCI/4Z level of theory; one more state of symmetry $^5\Pi$ has been considered correlating diabatically to V^+(^{5}P; 4s^{1}3d^3), 13 646.68 cm^{-1} higher, the sixth excited state of V^+.[16]

From the ground states of the neutral atoms, V(^{4}F; 4s^{2}3d^3)+Cl(^{2}P; 3s^{2}3p^5), stem 24 $^{2S+1}|\Lambda|$ states, triplets and quintets, namely ^{3,5}[$\Sigma^\pm$, Σ^-, Π(3), Δ(3), Φ(2),Γ]. The $M_L = \pm 1$ components of the Cl(^{2}P) interact repulsively or weakly attractively with the V ^{4}F(4s^{2}3d^3) term. On the contrary, the Cl atom in the $M_L = 0$ component with respect to the internuclear axis can easily accept an electron from the ^{4}F state of V by interacting with the diabatic ionic fragments V^++Cl^-. What is meant is succinctly indicated by the schemes below.

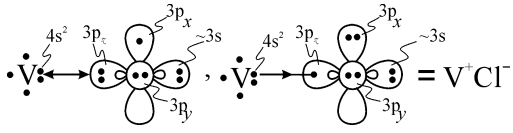

Therefore, eight states of the V^+Cl^- molecule with in situ V^+ atoms ^{5}F(4s^{1}3d^3), ^{3}F(4s^{1}3d^3), i.e., $^{3,5}\Sigma^-$, $^{3,5}\Pi$, $^{3,5}\Delta$, and $^{3,5}\Phi$, correlate to the neutral ground-state atoms V(^{4}F; 4s^{2}3d^3) + Cl(^{2}P, M_L=0). The three additional states $^5\Sigma^+$, $^5\Pi$, and $^5\Delta$ related to the ground ^{5}D(3d^4) state of V^+ correlate adiabatically to the neutral V(^{6}D; 4s^{1}3d^4) (the first excited state of neutral V atom 1977.22 cm^{-1} higher[16]) + Cl(^{2}P, M_L=0); the corresponding high-spin septets $^7\Sigma^+$, $^7\Pi$, and $^7\Delta$ are of repulsive nature. The discussion above is well captured in Figure 5 displaying the PECs of the 12 bound + 3 repulsive states examined here. The first 11 states shown in Figure 5 cover a MRCI(+Q)/4Z energy range of 8997 (7804) cm^{-1} reflecting the (experimental) splitting ΔE (^{3}F−^{5}D) = 8697.32 cm^{-1} of V^+.[16] In what follows we discuss first the sheaf of the first four quintets, then the four triplets, and then the three quintets.

A. States X $^5\Delta$, A $^5\Pi$, B $^5\Sigma^-$, and C $^5\Phi$. Following the experimentalists,[45,46] the lowest of the $^5\Delta$ states has been assigned to the ground state of VCl; our numerical results confirm this assignment but the next state ($^5\Pi$) could be considered as degenerate to X $^5\Delta$ within the accuracy of our calculations; see Table 6. The MRCI/4Z leading configurations ($|V^+\rangle$) and atomic equilibrium Mulliken distributions are given below.

$$|X^5\Delta\rangle_{A_1} \approx 0.95|3\sigma^1 2\pi_x^1 2\pi_y^1 1\delta_-^1\rangle$$

$$4s^{0.84}4p_z^{0.24}4p_{x,y}^{0.06}3d_{z^2}^{0.13}3d_{xz}^{1.01}3d_{yz}^{1.01}3d_{x^2-y^2}^{1.0}/Cl^{\delta-},\delta = 0.65$$

$$|A^5\Pi\rangle_{B_1} \approx 0.75|3\sigma^1 2\pi_y^1 1\delta_+^1 1\delta_-^1\rangle - 0.42|3\sigma^1 4\sigma^1 2\pi_x^1 1\delta_-^1\rangle + 0.41|3\sigma^1 4\sigma^1 2\pi_y^1 1\delta_+^1\rangle$$

$$4s^{0.86}4p_z^{0.28}4p_{x,y}^{0.05}3d_{z^2}^{0.47}3d_{xz}^{0.23}3d_{yz}^{0.83}3d_{x^2-y^2}^{0.81}3d_{xy}^{0.81}/Cl^{\delta-},\delta = 0.63$$

$$|B^5\Sigma^-\rangle_{A_2} \approx 0.90|3\sigma^1 4\sigma^1 1\delta_+^1 1\delta_-^1\rangle + 0.31|3\sigma^1 4\sigma^1 2\pi_x^1 2\pi_y^1\rangle$$

$$4s^{0.89}4p_z^{0.31}4p_{x,y}^{0.04}3d_{z^2}^{1.02}3d_{xz}^{0.15}3d_{yz}^{0.15}3d_{x^2-y^2}^{0.89}3d_{xy}^{0.89}/Cl^{\delta-},\delta = 0.65$$

$$|C^5\Phi\rangle_{B_1} \approx {}^1/_{\sqrt{2}}(|3\sigma^1 4\sigma^1 2\pi_y^1 1\delta_-^1\rangle + |3\sigma^1 4\sigma^1 2\pi_x^1 1\delta_+^1\rangle)$$

$$4s^{0.87}4p_z^{0.31}4p_{x,y}^{0.06}3d_{z^2}^{1.01}3d_{xz}^{0.53}3d_{yz}^{0.53}3d_{x^2-y^2}^{0.50}3d_{xy}^{0.50}/Cl^{\delta-},\delta = 0.67$$

The binding energy of the X $^5\Delta$ state at the MRCI(+Q)/4Z and RCCSD(T)/4Z levels is D_e = 96.1 (96.3) and 98.1 kcal/mol, respectively. Core (3s^{2}3p^6) and scalar relativistic effects at both MRCI and CC- methods are (a) of small importance, (b) of opposite sign, and (c) practically additive at the MRCI/4Z and RCCSD(T)/4Z methods. Thus, D_e[C-MRCI/C5Z+ DKH2(C-MRCI+Q/C4Z)] = 98−1.7 = 96.3 kcal/mol, as compared to 98.0 kcal/mol at the C-RCCSD(T)+DKH2/C5Z level, identical to the "plain" MRCI+Q/4Z and RCCSD(T)/4Z results. Adding +0.2 kcal/mol due to the core (2s^{2}2p^6) effects of Cl our best CC estimate is $D_0 = 98.0 + 0.2 - \omega_e/2 = 97.6$ kcal/mol in relatively good agreement with the thermochemical number of $D_0 = 101.9 \pm 2$ kcal/mol.[47]

Concerning the bond distance of the X $^5\Delta$ state, relativistic effects are of minor importance, −0.001 (MRCI) to −0.002 (CC) Å, but the core effects are as usual significant, −0.02 to −0.025 Å. Taking into account the Cl core effects (−0.004 Å) we obtain r_e = 2.255 (C-MRCI+Q/C5Z) − 0.004 = 2.251 Å and 2.234 − 0.004 = 2.230 Å at the C-RCCSD(T)+DKH2/C5Z level. The last number compares very favorably to the experimental value of 2.2145 Å.[46] Dipole moments obtained by the finite field approach converge to μ_{FF} = 4.1 (MRCI) and 4.3 (CC) D. Observe again the significant discrepancy between μ_{FF} and $\langle\mu\rangle$, the differences being 0.6−0.7 D.

The A $^5\Pi$ state can be formally considered as the first excited state of VCl. Our MRCI calculations at all levels point to a T_e energy separation of less than 1 kcal/mol, a dipole moment μ_{FF} = 3.4 D, and a bond distance r_e = 2.251 (C-MRCI+Q/C5Z). Taking relativistic effects into account at the C-MRCI+DKH2/C4Z level of theory (−0.003 Å) + core effects of the Cl atom (−0.003 or −0.004 Å), a better estimate for the equilibrium bond distance is r_e = 2.245 Å. We remind that no experimental data exist for the A $^5\Pi$ state.

The next two states, B $^5\Sigma^-$ and C $^5\Phi$, are well separated from the X $^5\Delta$ and A $^5\Pi$ pair with MRCI T_e values of about 1500 and 3400 cm^{-1}, respectively. Recommended dipole moments are 2.7 (B $^5\Sigma^-$) and 3.0 (C $^5\Phi$) D.

It is useful at this point to recall that in the isovalent species VF, the ground and first excited states are in reverse order as compared to VCl, that is, X $^5\Pi$ and A $^5\Delta$, with the latter about 3 kcal/mol higher.[3] As in VCl, a pair of well-separated states of symmetries B $^5\Sigma^-$ and C $^5\Phi$ follows, located at about

TABLE 6: Total Energies E (E_h), Dissociation Energies D_e (kcal/mol), Bond Distances r_e (Å), Harmonic and Anharmonic Frequencies ω_e, $\omega_e x_e$ (cm^{-1}), Rotational−Vibrational Constants α_e (cm^{-1}), Centrifugal Distortions $\bar{D}_e$ (cm^{-1}), Dipole Moments μ_e (D), and Energy Separations T_e (cm^{-1}) of $^{51}V^{35}Cl$

method/basis set[a]	$-E$	D_e	r_e	ω_e	$\omega_e x_e$	$\alpha_e \times 10^3$	$\bar{D}_e \times 10^7$	$\langle\mu\rangle$ (μ_{FF})[b]	T_e
				X $^5\Delta$					
MRCI/4Z	1402.782343	96.1	2.284	391	1.36	0.770	0.989	3.41 (4.02)	0.0
MRCI+*Q*	1402.808510	96.3	2.273	393	1.36	0.775	1.008		0.0
C-MRCI/C4Z	1403.125986	95.9	2.274	395	1.39	0.777	0.994	3.35 (4.10)	0.0
C-MRCI+*Q*	1403.197952	97.1	2.259	399	1.39	0.781	1.015		0.0
MRCI+DKH2/4Z	1409.439276	94.5	2.283	391				3.41 (3.98)	0.0
MRCI+DKH2+*Q*	1409.465451	94.6	2.272	393					0.0
C-MRCI+DKH2/C4Z	1409.782894	94.3	2.273	399				3.36 (4.06)	0.0
C-MRCI+DKH2+*Q*	1409.854717	95.4	2.258	399					0.0
MRCI/5Z	1402.789877	96.9	2.281	393	1.37	0.771	0.989	3.38 (3.99)	0.0
MRCI+*Q*/5Z	1402.816674	97.1	2.270	395	1.37	0.774	1.010		0.0
C-MRCI/C5Z	1403.139716	96.7	2.271	397				3.32 (4.08)	0.0
C-MRCI+*Q*/C5Z	1403.212953	98.0	2.255	402					0.0
RCCSD(T)/4Z	1402.818323	98.1	2.261	398	1.34	0.786	1.015	... (4.33)	0.0
C-RCCSD(T)/C4Z	1403.225358	99.4	2.240	407	1.42	0.795	1.029	... (4.43)	0.0
C^2-RCCSD(T)/C^2QZ	1403.564348	99.6	2.236	407	1.40	0.818	1.040	... (4.46)	0.0
RCCSD(T)+DKH2/4Z	1409.475002	95.7	2.259	412				... (4.18)	0.0
C-RCCSD(T)+DKH2/C4Z	1409.881864	96.7	2.238	409				... (4.32)	0.0
RCCSD(T)/5Z	1402.827272	99.1	2.257	404				... (4.29)	0.0
C-RCCSD(T)/C5Z	1403.241831	100.5	2.236	416				... (4.46)	0.0
C-RCCSD(T)+DKH2/C5Z	1409.898503	98.0	2.234	422				... (4.27)	0.0
MRCI+*Q*[c]			2.325	373				5.78	0.0
expt		101.9[d]	2.2145[e]	417.4[e]	1.0[f],3.5[e]	0.856(84)[f]			
				A $^5\Pi$					
MRCI/4Z	1402.780798	95.3	2.282	388	1.34	0.786	1.012	2.95 (3.37)	339
MRCI+*Q*	1402.807269	95.8	2.268	390	1.31	0.803	1.030		272
C-MRCI/C4Z	1403.124656	94.8	2.273	392	1.37	0.793	1.017	2.95 (3.43)	292
C-MRCI+*Q*	1403.196953	96.3	2.255	396	1.38	0.804	1.041		219
MRCI+DKH2/4Z	1409.437914	93.9	2.279	388				2.96 (3.34)	299
MRCI+DKH2+*Q*	1409.464379	94.3	2.266	391					235
C-MRCI+DKH2/C4Z	1409.781857	93.4	2.270	392				2.95 (3.42)	228
C-MRCI+DKH2+*Q*	1409.854058	94.7	2.253	394					145
MRCI/5Z	1402.788288	96.1	2.279	389	1.35	0.785	1.013	2.92 (3.34)	349
MRCI+*Q*	1402.815371	96.7	2.265	392	1.35	0.791	1.034		286
C-MRCI/C5Z	1403.138289	95.7	2.269	393				2.91 (3.40)	313
C-MRCI+*Q*	1403.211815	97.2	2.251	399					250
MRCI+*Q*[c]			2.326	366				3.93	517
				B $^5\Sigma^-$					
MRCI/4Z	1402.774993	92.1	2.305	376	1.28	0.759	1.013	2.85 (2.65)	1613
MRCI+*Q*	1402.801519	92.8	2.290	379	1.27	0.764	1.039		1534
C-MRCI/C4Z	1403.118926	91.3	2.297	379	1.30	0.768	1.016	3.00 (2.72)	1549
C-MRCI+*Q*	1403.191195	92.8	2.278	384	1.30	0.776	1.045		1483
MRCI+*Q*[c]			2.355	354					1587
				C $^5\Phi$					
MRCI/4Z	1402.767795	87.3	2.326	366	1.27	0.757	1.014	2.96 (2.97)	3193
MRCI+*Q*	1402.793721	87.2	2.314	368	1.28	0.759	1.035		3246
C-MRCI/C4Z	1403.111127	86.7	2.317	370	1.29	0.769	1.016	3.01 (3.06)	3261
C-MRCI+*Q*	1403.182685	87.6	2.302	373	1.29	0.776	1.039		3351
MRCI+*Q*[c]			2.374	346					3141
				a $^3\Pi$					
MRCI/4Z	1402.758830	81.6	2.272	392	1.35	0.773	1.017	2.68 (2.95)	5161
MRCI+*Q*	1402.786759	82.9	2.257	394	1.36	0.778	1.046		4774
C-MRCI/C4Z	1403.100872	79.9	2.261	397	1.37	0.780	1.027	2.67 (2.99)	5512
C-MRCI+*Q*	1403.174584	82.2	2.242	401	1.33	0.790	1.051		5129
MRCI+*Q*[c]			2.311	374					6418
				b $^3\Sigma^-$					
MRCI/4Z	1402.757898	81.4	2.256	384	1.24	0.761	1.107	2.50 (2.78)	5365
MRCI+*Q*	1402.786909	83.6	2.233	387	1.23	0.777	1.158		4741
C-MRCI/C4Z	1403.100110	79.4	2.247	388	1.24	0.762	1.107	2.55 (2.85)	5679
C-MRCI+*Q*	1403.174971	82.6	2.220	393	1.29	0.780	1.161		5044
MRCI+*Q*[c]			2.293	371					6169
				D $^5\Sigma^+$					
MRCI/4Z	1402.756263	88.8	2.356	348	1.13	0.846	1.018	7.56 (7.70)	5724
MRCI+*Q*	1402.789968	91.8	2.337	355	1.29	0.808	1.058		4070
C-MRCI/C4Z	1403.099419	88.0	2.342	352				7.62 (7.75)	5831
C-MRCI+*Q*	1403.181253	91.2	2.327	360					3665

TABLE 6: Continued

method/basis set[a]	$-E$	D_e	r_e	ω_e	$\omega_e x_e$	$\alpha_e \times 10^3$	$\bar{D}_e \times 10^7$	$\langle\mu\rangle$ (μ_{FF})[b]	T_e
MRCI+Q[c]			2.376	322					4097
				c $^3\Delta$					
MRCI/4Z	1402.755810	79.4	2.297	390	1.36	0.764	0.963	3.02 (3.57)	5823
MRCI+Q	1402.782835	80.1	2.287	391	1.36	0.768	0.982		5635
C-MRCI/C4Z	1403.097445	77.9	2.284	395	1.38	0.770	0.968	2.91 (3.57)	6264
C-MRCI+Q	1403.170006	79.5	2.272	398	1.38	0.774	0.989		6133
MRCI+Q[c]			2.340	372					7362
				d $^3\Phi$					
MRCI/4Z	1402.751429	77.0	2.261	372	1.19	0.770	1.161	2.92 (3.73)	6785
MRCI+Q	1402.780522	78.9	2.236	375	1.15	0.799	1.219		6143
C-MRCI/C4Z	1403.092715	75.1	2.253	377	1.21	0.769	1.158	2.87 (3.79)	7302
C-MRCI+Q	1403.167488	78.0	2.224	381	1.19	0.794	1.221		6686
MRCI+Q[c]			2.293	362					7470
				E $^5\Pi$					
MRCI/4Z	1402.747537	84.1	2.333	343	1.33	0.864	1.133	7.01 (6.39)	7639
MRCI+Q	1402.783541	87.8	2.326	344	1.22	0.865	1.130		5480
C-MRCI/C4Z	1403.093749	83.2	2.332	383				7.02 (6.44)	7075
C-MRCI+Q	1403.175524	87.0	2.324	378					4923
MRCI+Q[c]			2.332	369				4.10	10356
				F $^5\Delta$					
MRCI/4Z	1402.741350	79.3	2.388	328	1.23	0.842	1.060	6.40 (5.39)	8997
MRCI+Q	1402.772953	81.1	2.376	332	1.12	0.874	1.045		7804
C-MRCI/C4Z	1403.087005	78.7	2.386	339				6.49 (5.40)	8555
C-MRCI+Q	1403.164141	80.6	2.373	337					7421
MRCI+Q[c]			2.430	321				5.24	8494
expt[f]			2.2952	354.1[g]	1.0	0.9			7001.928(T_0)
				$^5\Pi$(3)					
MRCI/4Z	1402.721401		2.309	381	1.02	0.767	0.956	2.75 (2.55)	13375
MRCI+Q	1402.752215		2.283	390	0.59	0.844	0.967		12355
C-MRCI/C4Z	1403.067897		2.309	404				2.99 (2.75)	12729
C-MRCI+Q	1403.145934		2.286	396					11418

[a] +Q refers to the Davidson correction; C- and C^2- means that the $3s^23p^6$ and $2s^22p^6$ electrons of V and Cl, respectively, have been included in the CI. [b] $\langle\mu\rangle$ calculated as an expectation value, μ_{FF} through the finite field approach; field strength 5×10^{-5} au. [c] Reference 46; valence (12 e$^-$) MRCI+Q using 10-core electron relativistic pseudopotentials; separation energies as T_0. [d] Reference 47, thermochemistry, $D_0°$ value. [e] Reference 46, FTIR emission spectroscopy. [f] Reference 45, FTIR emission spectroscopy. [g] $\Delta G_{1/2}$ value.

2500 and 5600 cm^{-1} above the X $^5\Pi$ calculated at the same level of theory as in VCl.[3]

B. States a $^3\Pi$, b $^3\Sigma^-$, c $^3\Delta$, and d $^3\Phi$. The leading MRCI/4Z equilibrium configurations along with the atomic Mulliken populations of the four triplets are given below:

$$|a^3\Pi\rangle_{B_1} \approx 0.54|3\sigma^1 2\pi_y^1 1\bar{\delta}_+^1 1\delta_-^1\rangle - 0.30|3\sigma^1 4\sigma^1 2\bar{\pi}_y^1 1\delta_-^1\rangle - 0.28|3\sigma^2(2\pi_x^1 1\delta_+^1 - 2\pi_y^1 1\delta_-^1)\rangle - 0.26|3\sigma^1 4\sigma^1 2\pi_x^1 1\bar{\delta}_+^1\rangle - 0.24|4\bar{\sigma}^1 2\pi_y^1 1\delta_+^1 1\delta_-^1\rangle + 0.22|3\sigma^1 2\pi_y^1 1\delta_+^1 1\bar{\delta}_-^1\rangle$$

$$4s^{0.91}4p_z^{0.26}4p_{x,y}^{0.06}3d_{z^2}^{0.50}3d_{xz}^{0.26}3d_{yz}^{0.81}3d_{x^2-y^2}^{0.78}3d_{xy}^{0.78}/Cl^{\delta-}, \delta = 0.61$$

$$|b^3\Sigma^-\rangle_{A_2} \approx 0.68|3\sigma^1 4\sigma^1 1\bar{\delta}_+^1 1\delta_-^1\rangle - 0.37|3\sigma^1 4\bar{\sigma}^1 1\delta_+^1 1\delta_-^1\rangle + 0.34|3\sigma^2 1\delta_+^1 1\delta_-^1\rangle - 0.28|3\sigma^1 4\sigma^1 1\delta_+^1 1\bar{\delta}_-^1\rangle - 0.23|3\sigma^1 4\bar{\sigma}^1 2\pi_x^1 2\pi_y^1\rangle$$

$$4s^{0.96}4p_z^{0.26}4p_{x,y}^{0.06}3d_{z^2}^{1.01}3d_{xz}^{0.16}3d_{yz}^{0.16}3d_{x^2-y^2}^{0.89}3d_{xy}^{0.89}/Cl^{\delta-}, \delta = 0.60$$

$$|c^3\Delta\rangle_{A_1} \approx 0.77|3\sigma^1 2\pi_x^1 2\pi_y^1 1\bar{\delta}_+^1\rangle + 0.44|3\sigma^1 2\bar{\pi}_x^1 2\pi_y^1 1\delta_+^1\rangle + 0.31|3\sigma^1 2\pi_x^1 2\bar{\pi}_y^1 1\delta_+^1\rangle$$

$$4s^{0.87}4p_z^{0.26}4p_{x,y}^{0.06}3d_{z^2}^{0.12}3d_{xz}^{1.02}3d_{yz}^{1.02}3d_{x^2-y^2}^{1.0}/Cl^{\delta-}, \delta = 0.64$$

$$|d^3\Phi\rangle_{B_1} \approx 0.46|3\sigma^2(2\pi_x^1 1\delta_+^1 + 2\pi_y^1 1\delta_-^1)\rangle - 0.38|3\sigma^1 4\sigma^1 2\pi_x^1 1\bar{\delta}_+^1\rangle + 0.27|3\sigma^1(4\sigma^1 2\bar{\pi}_y^1 - 4\bar{\sigma}^1 2\pi_y^1)1\delta_-^1\rangle$$

$$4s^{0.99}4p_z^{0.24}4p_{x,y}^{0.06}3d_{z^2}^{1.0}3d_{xz}^{0.54}3d_{yz}^{0.54}3d_{x^2-y^2}^{0.50}3d_{xy}^{0.50}/Cl^{\delta-}, \delta = 0.61$$

Notice the extreme multireference character of the triplets correlating adiabatically to the ground neutral atoms, V(^{4}F) + Cl(^{2}P; M_L=0). From Figure 5 and Table 6 it is seen that the a $^3\Pi$ and b $^3\Sigma^-$ states are degenerate, the tagging a and b being only formal. The next two states, c $^3\Delta$ and d $^3\Phi$, are separated by about 500 cm^{-1} at both the MRCI+Q/4Z and C-MRCI+Q/C4Z level. It should be stressed here that all our splittings are qualitative; for instance, whereas the D $^5\Sigma^+$ state correlating to the first excited neutral atoms V(^{6}D) + Cl(^{2}P; M_L=0) is located between the b $^3\Sigma^-$ and c $^3\Delta$ states at the MRCI/4Z or C-MRCI/C4Z level, the Davidson correction relocates it below the a $^3\Pi$ and above the C $^5\Phi$ state. Finally, recommended dipole moments μ_{FF} are 3.0 (a $^3\Pi$), 2.8 (b $^3\Sigma^-$), 3.6 (c $^3\Delta$), and 3.8 (d $^3\Phi$) D.

C. States D $^5\Sigma^+$, E $^5\Pi$, F $^5\Delta$, and $^5\Pi$(3). As was already discussed in the introduction of Section 6, the D $^5\Sigma^+$, E $^5\Pi$, and F $^5\Delta$ states correlate adiabatically to the first excited-state of V(^{6}D; $4s^13d^4$) + Cl(^{2}P; M_L=0) (see Figure 5), but diabatically to V$^+$(^{5}D; $3d^4$) + Cl$^-$(^{1}S). At the MRCI(+Q)/4Z level the asymptotic supermolecule difference is $\Delta E(^6D-^4F) = 3205$ (2294) cm^{-1} in fair agreement with the experimental value of 1977.22 cm^{-1}. The $^5\Pi$(3) state, well separated from the D, E, and F quintets, is rather related to the ^{5}P($4s^13d^4$) of V$^+$, 13 646.68 cm^{-1} above the ground state of V$^+$(^{5}D; $3d^4$).[16]

The equilibrium leading MRCI/4Z configurations and corresponding Mulliken populations are ($|V^+\rangle$)

$$|D^5\Sigma^+\rangle_{A_1} \approx 0.96|2\pi_x^1 2\pi_y^1 1\delta_+^1 1\delta_-^1\rangle$$

$$4s^{0.09}4p_z^{0.04}4p_{x,y}^{0.06}3d_{z^2}^{0.07}3d_{xz}^{1.0}3d_{yz}^{1.0}3d_{x^2-y^2}^{1.0}3d_{xy}^{1.0}/Cl^{\delta-},\delta = 0.73$$

$$|E^5\Pi\rangle_{B_1} \approx 0.80|3\sigma^1 4\sigma^1 2\pi_y^1 1\delta_-^1\rangle + 0.39|3\sigma^1 2\pi_x^1 1\delta_+^1 1\delta_-^1\rangle + 0.22|4\sigma^1 2\pi_y^1 1\delta_+^1 1\delta_-^1\rangle + 0.22|3\sigma^1 4\sigma^1 2\pi_x^1 1\delta_+^1\rangle$$

$$4s^{0.23}4p_z^{0.09}4p_{x,y}^{0.05}3d_{z^2}^{0.97}3d_{xz}^{0.09}3d_{yz}^{0.95}3d_{x^2-y^2}^{0.94}3d_{xy}^{0.94}/Cl^{\delta-},\delta = 0.72$$

$$|F^5\Delta\rangle_{A_1} \approx 0.95|4\sigma^1 2\pi_x^1 2\pi_y^1 1\delta_-^1\rangle$$

$$4s^{0.90}4p_z^{0.15}4p_{x,y}^{0.06}3d_{z^2}^{0.91}3d_{xz}^{1.0}3d_{yz}^{1.0}3d_{xy}^{1.0}/Cl^{\delta-},\delta = 0.76$$

$$|^5\Pi(3)\rangle_{B_1} \approx 0.48|3\sigma^1 4\sigma^1 2\pi_y^1 1\delta_-^1\rangle - 0.48|4\sigma^1 2\pi_y^1 1\delta_+^1 1\delta_-^1\rangle - 0.48|3\sigma^1 4\sigma^1 2\pi_x^1 1\delta_+^1\rangle - 0.45|3\sigma^1 2\pi_y^1 1\delta_+^1 1\delta_-^1\rangle$$

$$4s^{0.71}4p_z^{0.32}4p_{x,y}^{0.05}3d_{z^2}^{0.69}3d_{xz}^{0.30}3d_{yz}^{0.76}3d_{x^2-y^2}^{0.74}3d_{xy}^{0.74}/Cl^{\delta-},\delta = 0.66$$

Opening diabatically the $^5\Pi(3)$ state it ends up to $V^+(^5P; 4s^13d^3)$, whereas the diabatic opening of the D, E, and F quintets leads to $V^+(^5D; 3d^4)$, the ground state of V^+. The MRCI(+Q)/4Z splitting $\Delta E(^5P-{}^5D)$ calculated at 100 Å is 13 120 (14676) cm^{-1} in fair agreement with the experimental value of 13 646.68 cm^{-1}.[16] Obviously the E $^5\Pi$ and $^5\Pi(3)$ states interact relatively strongly around equilibrium, thus their multireference character.

A comment is needed for the dipole moments of those four quintets. Note the high dipole moment values of the D, E, and F quintets (μ_{FF}), namely 7.7, 6.4, and 5.4 D, respectively, while it drops to about 2.6−2.7 D for the $^5\Pi(3)$ state. The reason is the different ancestry of the D, E, and F states from the $^5\Pi(3)$, that is $V^+(3d^4)$ vs $V^+(4s^13d^3)$. The $4s^{0.71}4p_z^{0.32}3d_{z^2}^{0.69}$ strong hybridization in the $^5\Pi(3)$ state results in a charge distribution on the "back" of the in situ V^+ atom, hence the smaller dipole moment.

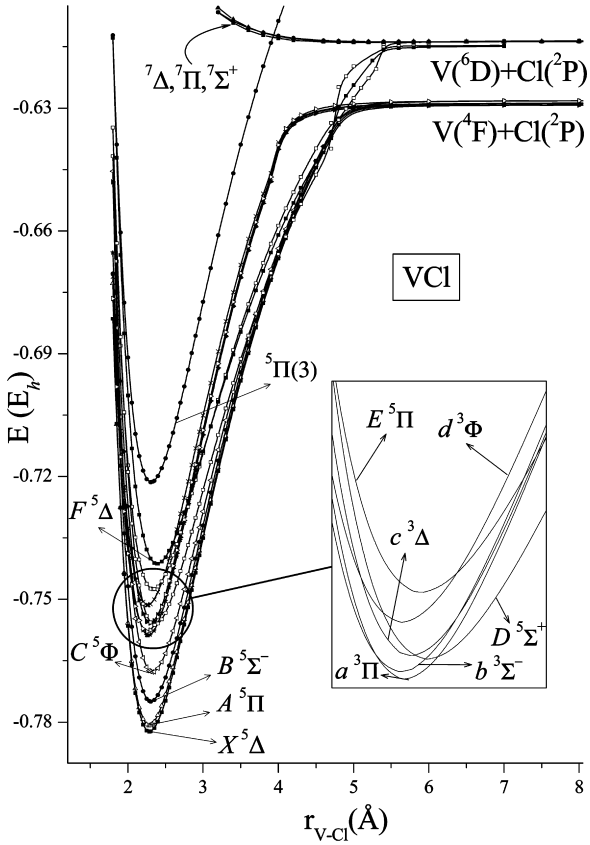

Figure 5. MRCI/4Z potential energy curves of the VCl molecule. Energies are shifted by +1402 E_h.

Finally, the available experimental results[46] for the F $^5\Delta$ state r_e, ω_e, $\omega_e x_e$, α_e, and T_{00} compare favorably with our theoretical predictions (Table 6).

7. Results and Discussion on CrCl

The first spectroscopic observation on CrCl in the region 15 600−17 500 cm^{-1} was obtained by Rao and Rao in 1949.[49] The flame photometric dissociation energy of CrCl, $D_0^o = 86.5 \pm 6$ kcal/mol, was measured by Bulewicz et al. in 1961,[50] whereas a similar mass spectrometric value, $D_0^o = 85.6 \pm 1.2$ kcal/mol, was reported by Milushin and Gorokhov 27 years later.[51] Oike et al. recorded for the first time the pure rotational spectrum of the X $^6\Sigma^+$ state of $^{52}Cr^{35}Cl$ reporting several fine structure constants, and a bond distance $r_0 = 2.1971$ Å.[52] More recently, Bencheikh et al. analyzed the A $^6\Sigma^+ \rightarrow$ X $^6\Sigma^+$ system of CrCl and CrF by high-resolution near-infrared spectroscopy,[53] whereas Oike and co-workers examined the rotational spectrum of $^{52}Cr^{35}Cl$ and $^{52}Cr^{37}Cl$ reporting highly accurate B_0 values;[54] their results will be compared with ours later on. In addition, the B $^6\Pi-$X $^6\Sigma^+$ band system of the CrCl radical has been recorded by Koivisto et al.[55] by Fourier transform spectroscopy in the region 6900−11 700 cm^{-1} (see below). Finally, in a recent work, Hildenbrand gives thermochemical dissociation energies for the metal monochlorides MCl, M = Cr, Mn, Fe, Co, and Ni;[33b] in particular, $D_0^o = 90.0 \pm 1.3$ kcal/mol for CrCl.

We are aware of four theoretical publications on CrCl.[53,55−57] In ref 53 the authors report density functional theory (DFT) results for the first seven states of CrCl, while Nielsen and Allendorf[57] performed CCSD(T)/[7s6p4d3f2g/$_M$ aug-cc-pVQZ/$_{Cl}$]//DFT(B3LYP)/6-311+G(d) calculations on the MX (M = Cr, Mn, Fe; X = F, Cl) systems. Koivisto et al.[55] obtained r_e, ω_e, and T_e values for the seven lowest states of CrCl through the RAS (restrictive active space-SCF)-MRCI method; however, the details of their calculations are not very clear.

The most extensive calculations so far on CrCl are those of Harrison and Hutchison[56] who performed MRCI(+Q) and RCCSD(T) calculations using a contracted [(ANO) 7s6p4d3f2g/$_{Cr}$ aug-cc-pVQZ/$_{Cl}$] basis set, taking also into account the semicore correlation of $Cr(3s^23p^6)$ and scalar relativistic effects through the Cowan−Griffin approach. They have studied the first seven states of CrCl around equilibrium focusing on r_e, ω_e, μ_e, T_e reporting as well the dissociation energy D_0 for the X $^6\Sigma^+$ state. Their results, shown in Table 7 for easy comparison, are very similar to ours.

Presently, we have constructed CrCl PECs for 27 states, four of which are of repulsive nature; the symmetries of the latter are $^8\Sigma^+(1)$, $^6\Sigma^+(3)$, and $^8\Pi$, $^8\Sigma^+(2)$ correlating to $Cr(^7S)$, $Cr(^5D; 4s^23d^4)$, and $Cr(^7P; 3d^54p^1) + Cl(^2P, M_L=0)$, respectively; see Figure 6. The 23 states are all bound, crowded in an energy range of about 3.8 eV. As can be seen from Figure 6 and Table 7, they are grouped in two bundles of 7 and 16 states, the latter having a density of 0.046 eV (≈1 kcal/mol) per state at the MRCI+Q/4Z level. We discuss the first seven states, followed by a very brief exposition for the remaining 16 higher ones.

A. States X $^6\Sigma^+$, A $^6\Pi(1)$, B$^6\Sigma^+(2)$, a $^4\Sigma^+(1)$, C $^6\Delta(1)$, b $^4\Pi(1)$, and c $^4\Delta(1)$. As expected, CrCl is adequately described around equilibrium as ionic, Cr^+Cl^-, with 0.6−0.7 e^- migrating from Cr to Cl ($^2P; M_L=0$) according to the Mulliken populations (vide infra). Following the same line of thought as before, we can rationalize the (diabatic) ancestry of the seven states above

TABLE 7: Total Energies E (E_h), Dissociation Energies D_e (kcal/mol), Bond Distances r_e (Å), Harmonic and Anharmonic Frequencies ω_e, $\omega_e x_e$ (cm^{-1}), Rotational−Vibrational Constants α_e (cm^{-1}), Centrifugal Distortions $\bar{D}_e$ (cm^{-1}), Dipole Moments μ_e (D), and Energy Separations T_e (cm^{-1}) of $^{52}Cr^{35}Cl$

method/basis set[a]	−E	D_e	r_e	ω_e	$\omega_e x_e$	$\alpha_e \times 10^3$	$\bar{D}_e \times 10^7$	$\langle\mu\rangle$ (μ_{FF})[b]	T_e
			X $^6\Sigma^+$						
MRCI/4Z	1503.260183	85.0	2.240	380	1.78	1.003	1.178	6.51 (6.38)	0.0
MRCI+*Q*	1503.294804	88.9	2.235	378	2.19	1.083	1.206		0.0
C-MRCI/C4Z	1503.617387	80.3	2.225	391	2.42	1.138	1.161	5.29 (6.70)	0.0
C-MRCI+*Q*	1503.696496	84.3	2.213	390	1.71	0.937	1.197		0.0
MRCI+DKH2/4Z	1510.963603	83.7	2.214	393				4.83 (5.97)	0.0
MRCI+DKH2+*Q*	1510.996223	86.3	2.204	385					0.0
C-MRCI+DKH2/C4Z	1511.324882	81.6	2.210	400				4.85 (6.02)	0.0
C-MRCI+DKH2+*Q*	1511.403630	85.1	2.196	391					0.0
MRCI/5Z	1503.264689	83.4	2.226	390	2.31	1.067	1.161	5.25 (6.62)	0.0
MRCI+*Q*	1503.298425	86.4	2.217	400	2.64	1.102	1.190		0.0
C-MRCI/C5Z	1503.633043	80.9	2.221	393	2.11	1.001	1.160	5.25 (6.70)	0.0
C-MRCI+*Q*	1503.713649	85.0	2.209	391	2.01	1.012	1.193		0.0
MRCI+DKH2/5Z	1510.972132	84.6	2.211	410	2.10	0.931	1.095	4.80 (5.94)	0.0
MRCI+DKH2+*Q*	1511.005542	87.2	2.201	411	2.14	0.939	1.120		0.0
C-MRCI+DKH2/C5Z	1511.340705	82.1	2.206	413	2.12	0.930	1.093	4.82 (6.01)	0.0
C-MRCI+DKH2+*Q*	1511.420961	85.8	2.193	415	1.82	0.944	1.124		0.0
RCCSD(T)/4Z	1503.303153	90.0	2.229	492				... (7.65)	0.0
C-RCCSD(T)/C4Z	1503.731324	89.2	2.214	389	1.73	0.692	1.189	... (6.08)	0.0
RCCSD(T)+DKH2/4Z	1511.006979	86.7	2.203	413				... (5.94)	0.0
C-RCCSD(T)+DKH2/C4Z	1511.433095	85.9	2.179	417				... (3.78)	0.0
RCCSD(T)/5Z	1503.313055	91.0	2.224	384	2.83		1.197	... (6.23)	0.0
C-RCCSD(T)/C5Z	1503.750166	90.1	2.208	396	2.36		1.157	... (6.06)	0.0
RCCSD(T)+DKH2/5Z	1511.017059	85.2	2.196	412	1.54	0.873	1.129	... (5.45)	0.0
C-RCCSD(T)+DKH2/C5Z	1511.451927	86.9	2.173	434	1.66	0.877	1.083	... (5.75)	0.0
C-MRCI+CG+*Q*/ANO[c]		83.7[d]	2.206	405				6.42	0.0
expt		90.0 ±1.3[e]	2.193952(2)[f]	396.6621[g]		0.972[h]	1.1835[g]		
			A $^6\Pi(1)$[i]						
MRCI/4Z	1503.225688	89.4	2.276	382	1.31	0.780	1.033	2.80 (2.82)	7571
MRCI+*Q*	1503.255316	89.8	2.263	385	1.32	0.787	1.055		8667
C-MRCI/C4Z	1503.586580	88.7	2.273	386				2.89 (2.98)	6761
C-MRCI+*Q*	1503.661537	89.8	2.258	396					7673
MRCI+DKH2/4Z	1510.936533	87.9	2.272	393				2.71 (2.77)	5941
MRCI+DKH2+*Q*	1510.966332	88.2	2.258	385					6560
C-MRCI+DKH2/C4Z	1511.297722	87.2	2.268	385				2.89 (2.87)	5961
C-MRCI+DKH2+Q	1511.372728	88.1	2.252	376					6782
MRCI/5Z	1503.233950	90.1	2.273	386				2.77 (2.84)	6746
MRCI+*Q*	1503.264341	90.6	2.258	378					7481
C-MRCI/C5Z	1503.601992	89.4	2.269	385				2.86 (2.95)	6815
C-MRCI+*Q*	1503.678400	90.6	2.252	376					7736
MRCI+DKH2/5Z	1510.944962	88.6	2.273	362				2.80 (2.89)	5963
MRCI+DKH2+*Q*	1510.975460	89.0	2.257	355					6602
C-MRCI+DKH2/C5Z	1511.313321	87.9	2.265	386	1.38	0.788	1.042	2.86 (2.95)	6010
C-MRCI+DKH2+*Q*	1511.389826	89.0	2.248	390	1.34	0.811	1.067		6833
RCCSD(T)/4Z	1503.263202	90.8	2.259	385	1.22	0.805	1.065	... (2.48)	8768
C-RCCSD(T)/C4Z	1503.687585	89.2	2.244	391	1.54	0.825	1.074	... (2.41)	9599
RCCSD(T)+DKH2/4Z	1510.974266	87.1	2.254	381				... (2.48)	7180
RCCSD(T)/5Z	1503.272915	91.6	2.254	385	1.02	0.860	1.073	... (2.45)	8810
C-RCCSD(T)/C5Z	1503.705805	90.1	2.239	393	1.30	0.814	1.080	... (2.35)	9736
RCCSD(T)+DKH2/5Z	1510.984176	89.7	2.250	389	1.58	0.833	1.071	... (2.45)	7217
C-MRCI+CG+*Q*/ANO[c]			2.247	394				2.86	7377
expt			2.23[j]						8870[j]
			B $^6\Sigma^+(2)$[k]						
MRCI/4Z	1503.223939	82.8	2.317	381	1.24	0.681	0.958	3.14 (3.23)	7955
MRCI+*Q*	1503.255890	84.7	2.303	386	0.86	0.698	0.965		8541
C-MRCI/C4Z	1503.589005	84.0	2.322	384	1.49	0.556	0.931	4.79 (2.89)	6229
C-MRCI+*Q*	1503.668107	87.8	2.307	389	0.30	0.603	0.941		6231
MRCI/5Z	1503.221520	83.2	2.308	377				3.39 (3.06)	9475
MRCI+*Q*	1503.251097	86.4	2.298	371					10387
MRCI+DKH2/5Z	1510.944423	88.4	2.330	383				5.24 (2.86)	6081
MRCI+DKH2+*Q*	1510.979499	91.6	2.319	382					5716
C-MRCI+CG+*Q*/ANO[c]			2.302	382				3.35	7878
expt[g]			2.270	379.39			0.12(10)		9469
			a $^4\Sigma^+(1)$[k]						
MRCI/4Z	1503.212091	75.6	2.242	407	1.40	0.786	0.999	2.79 (2.42)	10555
MRCI+*Q*	1503.242151	76.3	2.230	409	1.41	0.792	1.019		11556
C-MRCI+CG+*Q*/ANO[c]			2.214	422				3.41	11309

TABLE 7: Continued

method/basis set[a]	$-E$	D_e	r_e	ω_e	$\omega_e x_e$	$\alpha_e \times 10^3$	$\bar{D}_e \times 10^7$	$\langle\mu\rangle$ (μ_{FF})[b]	T_e
				C $^6\Delta(1)$[i]					
MRCI/4Z	1503.208446	82.3	2.314	374	2.75	1.120	0.968	3.28 (3.46)	10865
MRCI+Q	1503.240678	82.3	2.301	377	1.16	0.852	1.038		11748
C-MRCI+CG+Q/ANO[c]			2.284	379				3.96	10063
				b $^4\Pi(1)$[i]					
MRCI/4Z	1503.202271	74.7	2.234	389	1.29	0.771	1.116	2.47 (2.97)	11355
MRCI+Q	1503.234428	76.7	2.212	392	1.28	0.781	1.166		13251
C-MRCI+CG+Q/ANO[c]			2.192	404				2.52	12407
				c $^4\Delta(1)$[i]					
MRCI/4Z	1503.191013	68.2	2.258	377	1.30	0.784	1.133	3.23 (3.90)	15181
MRCI+Q	1503.221813	69.0	2.244	379	1.29	0.791	1.191		16020
C-MRCI+CG+Q/ANO[c]			2.160	388				3.26	14750
				$^4\Gamma(1)$					
MRCI/4Z	1503.151005	94.8	2.216	411	1.38	0.814	1.050	2.90 (3.71)	23962
MRCI+Q	1503.183466	95.9	2.199	415	1.42	0.822	1.078		24436
				$^4\Sigma^-(1)$					
MRCI/4Z	1503.147593	92.5	2.223	407	1.44	0.814	1.049	2.85 (3.50)	24711
MRCI+Q	1503.181073	93.3	2.206	411	1.42	0.809	1.078		24961
				$^4\Phi(1)$					
MRCI/4Z	1503.146755	92.4	2.223	407	1.36	0.810	1.053	2.72 (3.67)	24894
MRCI+Q	1503.179297	93.4	2.204	411	1.44	0.821	1.083		25351
				$^4\Delta(2)$					
MRCI/4Z	1503.144344	90.9	2.217	402	1.38	0.830	1.092	3.00 (3.98)	25423
MRCI+Q	1503.178235	92.8	2.193	409	1.45	0.844	1.128		25584
				$^4\Pi(2)$					
MRCI/4Z	1503.140061	87.8	2.242	385	1.41	0.728	1.116	2.54 (2.93)	26364
MRCI+Q	1503.173432	89.3	2.221	388	2.20	0.720	1.165		26368
				$^4H(1)$					
MRCI/4Z	1503.139477	87.2	2.260	387	1.27	0.774	1.049	2.51 (2.53)	26492
MRCI+Q	1503.170996	87.7	2.244	388	0.71	0.709	1.086		27173
				$^4\Pi(3)$					
MRCI/4Z	1503.135685	92.3	2.246	379	1.12	0.733	1.143	2.57 (2.83)	27324
MRCI+Q	1503.168640	97.0	2.221	381	0.82	0.767	1.199		26690
				$^4\Sigma^+(2)$					
MRCI/4Z	1503.134035	89.5	2.205	411	1.41	0.823	1.082	3.01 (4.20)	27686
MRCI+Q	1503.169329	95.7	2.182	417	1.46	0.837	1.116		25539
				$^4\Delta(3)$					
MRCI/4Z	1503.133589	96.7	2.252	391	1.29	0.787	1.051	2.61 (2.51)	27784
MRCI+Q	1503.166766	101.4	2.234	394	1.29	0.797	1.086		28101
				$^4\Sigma^-(2)$					
MRCI/4Z	1503.133206	84.2	2.257	381	1.31	0.790	1.093	2.85 (3.01)	27868
MRCI+Q	1503.166289	85.5	2.232	385	1.34	0.783	1.145		28206
				$^2\Gamma(1)$					
MRCI/4Z	1503.131861	82.0	2.220	409	1.36	0.797	1.044	2.77 (3.57)	28163
MRCI+Q	1503.163713	82.9	2.208	412	1.61	0.783	1.068		28771
				$^2\Phi(1)$					
MRCI/4Z	1503.130652	85.4	2.212	404	1.46	0.742	1.098	2.69 (3.49)	28429
MRCI+Q	1503.164254	83.6	2.192	404	1.52	0.706	1.159		28652
				$^2H(1)$					
MRCI/4Z	1503.128667	79.9	2.193	386	1.14	0.755	1.264	2.84 (4.19)	28864
MRCI+Q	1503.163126	82.5	2.164	389	0.84	0.764	1.354		28900
				$^2\Delta(1)$					
MRCI/4Z	1503.127033	79.3	2.217	399	1.54	0.730	1.107	2.51 (2.97)	29223
MRCI+Q	1503.159698	80.7	2.201	401	2.04	0.701	1.150		29652
				$^2\Pi(1)$					
MRCI/4Z	1503.126912	78.8	2.203	388	1.25	0.718	1.216	2.60 (3.56)	29250
MRCI+Q	1503.162376	81.2	2.191	385	0.71	0.759	1.309		29065
				$^2\Pi(2)$					
MRCI/4Z	1503.121981	76.1	2.217	386	1.22	0.794	1.187	2.59 (3.11)	30332
MRCI+Q	1503.156698	78.8	2.170	403					30311

[a] +Q refers to the Davidson correction; C- means that the $3s^23p^6$ electrons of Cr have been included in the CI. [b] $\langle\mu\rangle$ calculated as an expectation value, μ_{FF} through the finite field approach; field strength 5×10^{-5} au. [c] Reference 56, scalar relativistic effects through the Cowan−Griffin (CG) approach; ANO = [7s6p4d3f2g/$_{Cr}$ aug-cc-pVQZ/$_{Cl}$] for the valence MRCI calculations and [8s8p6d4f2g/$_{Cr}$ aug-cc-pVQZ/$_{Cl}$] for the C-MRCI; dipole moments calculated at the C-MRCI level. [d] D_0 indirectly obtained through the RCCSD(T) method; see ref 56. [e] D_0°; ref 33b. [f] Reference 54. [g] Reference 53. [h] Reference 55. [i] D_e with respect to adiabatic fragments Cr(^{5}D; $4s^23d^4$)+Cl(^{2}P). [j] Estimated T_0 and r_0 values; ref 55. [k] D_e with respect to Cr(^{5}S; $4s^13d^5$)+Cl(^{2}P).

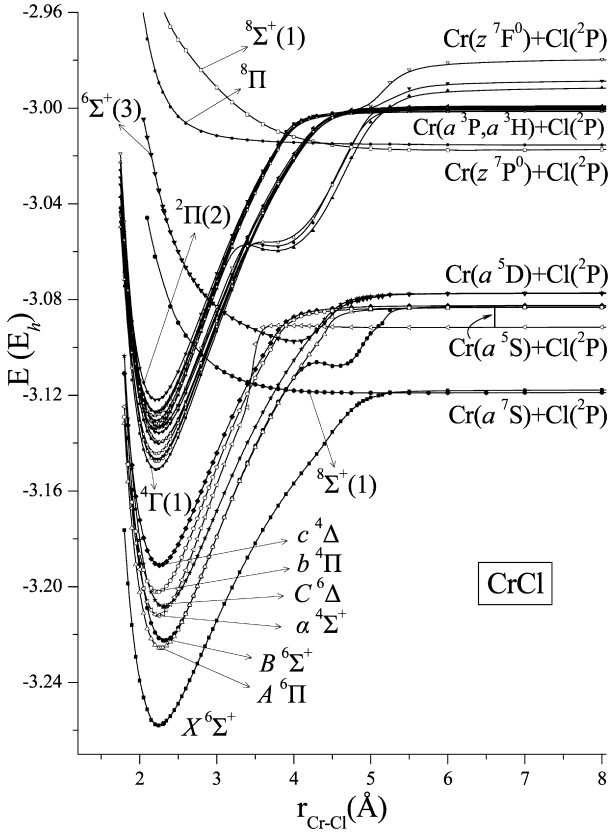

Figure 6. MRCI/4Z potential energy curves of the CrCl molecule. Energies are shifted by +1500 E_h.

from the Cr^+ terms in the field of $Cl^-(^1S)$. Indeed, the first three states of Cr^+ are $^6(3d^5)$, $^6D(4s^13d^4)$, and $^4D(4s^13d^4)$ with atomic energy separations of 0.0, 12 277.87, and 19 828.03 cm^{-1}.[16] Along the internuclear axis the atomic terms are projected to $^6S \rightarrow X\ ^6\Sigma^+$, $^6D \rightarrow A\ ^6\Pi(1)$, $B\ ^6\Sigma^+(2)$, $C\ ^6\Delta(1)$, and $^4D \rightarrow a\ ^4\Sigma^+(1)$, $b\ ^4\Pi(1)$, $c\ ^4\Delta(1)$, this ordering being the results of MRCI/4Z calculations (but see below). These seven $^{2S+1}|\Lambda|$ states correlate adiabatically to Cr (^7S; $4s^13d^5$) ($X\ ^6\Sigma^+$), Cr (^5D; $4s^23d^4$) [$A\ ^6\Pi(1)$, $C\ ^6\Delta(1)$, $b\ ^4\Pi(1)$, $c\ ^4\Delta(1)$], Cr(^5S; $4s^13d^5$) [$B\ ^6\Sigma^+(2)$, $a\ ^4\Sigma^+(1)$] + Cl(^2P; M_L=0); see Figure 6. Their main equilibrium MRCI configurations ($|Cr^+\rangle$) and atomic Mulliken distributions follow:

$$|X^6\Sigma^+\rangle_{A_1} \approx |[(0.72)3\sigma^1 - (0.60)4\sigma^1]2\pi_x^1 2\pi_y^1 1\delta_+^1 1\delta_-^1\rangle$$

$$4s^{0.46}4p_z^{0.05}4p_{x,y}^{0.06}3d_{z^2}^{0.71}3d_{xz}^{1.01}3d_{yz}^{1.01}3d_{x^2-y^2}^{1.0}3d_{xy}^{1.0}/Cl^{\delta-}, \delta = 0.69$$

$$|A^6\Pi(1)\rangle_{B_1} \approx 0.95|3\sigma^1 4\sigma^1 2\pi_x^1 1\delta_+^1 1\delta_-^1\rangle$$

$$4s^{0.86}4p_z^{0.31}4p_{x,y}^{0.05}3d_{z^2}^{1.02}3d_{xz}^{0.05}3d_{yz}^{1.01}3d_{x^2-y^2}^{1.0}3d_{xy}^{1.0}/Cl^{\delta-}, \delta = 0.67$$

$$|B^6\Sigma^+(2)\rangle_{A_1} \approx |[(0.72)4\sigma^1 + (0.60)3\sigma^1]2\pi_x^1 2\pi_y^1 1\delta_+^1 1\delta_-^1\rangle$$

$$4s^{0.53}4p_z^{0.32}4p_{x,y}^{0.04}3d_{z^2}^{0.36}3d_{xz}^{1.01}3d_{yz}^{1.01}3d_{x^2-y^2}^{1.0}3d_{xy}^{1.0}/Cl^{\delta-}, \delta = 0.70$$

$$|C^6\Delta(1)\rangle_{A_1} \approx 0.95|3\sigma^1 4\sigma^1 2\pi_x^1 2\pi_y^1 1\delta_-^1\rangle$$

$$4s^{0.89}4p_z^{0.31}4p_{x,y}^{0.04}3d_{z^2}^{1.02}3d_{xz}^{1.01}3d_{yz}^{1.01}3d_{xy}^{1.0}/Cl^{\delta-}, \delta = 0.69$$

$$|a^4\Sigma^+(1)\rangle_{A_1} \approx |3\sigma^1 2\pi_x^1 2\pi_y^1[(0.75)1\bar{\delta}_+^1 1\delta_-^1 + (0.24)1\delta_+^1 1\bar{\delta}_-^1]\rangle + |3\sigma^1[(0.42)2\bar{\pi}_x^1 2\pi_y^1 + (0.30)2\pi_x^1 2\bar{\pi}_y^1]1\delta_+^1 1\delta_-^1\rangle$$

$$4s^{0.87}4p_z^{0.28}4p_{x,y}^{0.04}3d_{z^2}^{0.13}3d_{xz}^{1.01}3d_{yz}^{1.01}3d_{x^2-y^2}^{0.99}3d_{xy}^{0.99}/Cl^{\delta-}, \delta = 0.63$$

$$|b^4\Pi(1)\rangle_{B_1} \approx |[(0.64)3\sigma^2 - (0.42)4\sigma^2]2\pi_y^1 1\delta_+^1 1\delta_-^1\rangle + |3\sigma^1 4\sigma^1[(0.37)2\bar{\pi}_y^1 1\delta_+^1 1\delta_-^1 + (0.28)2\pi_y^1 1\delta_+^1 1\bar{\delta}_-^1]\rangle$$

$$4s^{0.94}4p_z^{0.27}4p_{x,y}^{0.06}3d_{z^2}^{1.02}3d_{xz}^{0.06}3d_{yz}^{1.02}3d_{x^2-y^2}^{1.0}3d_{xy}^{1.0}/Cl^{\delta-}, \delta = 0.62$$

$$|c^4\Delta(1)\rangle_{A_2} \approx |3\sigma^1 4\sigma^1 2\pi_x^1[(0.59)2\pi_y^1 1\bar{\delta}_+^1 + (0.21)2\bar{\pi}_y^1 1\delta_+^1]\rangle + |[(0.54)3\sigma^2 - (0.27)4\sigma^2]2\pi_x^1 2\pi_y^1 1\delta_+^1\rangle + |3\sigma^1[(0.27)4\sigma^1 2\bar{\pi}_x^1 + (0.21)4\bar{\sigma}^1 2\pi_x^1]2\pi_y^1 1\delta_+^1\rangle$$

$$4s^{0.97}4p_z^{0.25}4p_{x,y}^{0.06}3d_{z^2}^{1.02}3d_{xz}^{1.02}3d_{yz}^{1.02}3d_{x^2-y^2}^{1.0}/Cl^{\delta-}, \delta = 0.65$$

It is to be reminded at this point that experimental results are limited to the first three states of CrCl, X $^6\Sigma^+$, A $^6\Pi(1)$, and E $^6\Sigma^+(2)$; see Table 7. As can be seen from Figure 6 (or Table 7), states A $^6\Pi(1)$, B $^6\Sigma^+$, and a $^4\Sigma^+(1)$, C $^6\Delta(1)$ are very close in energy, their given relative ordering being only formal. Notice also that with the exception of the A $^6\Pi(1)$ and $C^6\Delta(1)$, the rest of the states are of multireference character.

The bonding in the X-state of CrCl is clearly caused by a charge transfer of about 0.7 e^- from the 4s orbital of Cr (^7S; $4s^13d^5$) to the $3p_z$ orbital of Cl (^2P; M_L=0), due to the avoided crossing at 5.15 Å; Figure 6. However, and according to the composition of the natural CASSCF 3σ and 4σ orbitals, it is suggested that the in situ Cr^+ entity can be described by the composition $|Cr^+;X\ ^6\Sigma^+\rangle \approx 0.72|^6D;\ 4s^13d^4\rangle - 0.60|^6S;\ 3d^5\rangle$.

The corresponding Cr^+ in situ composition for the complementary B $^6\Sigma^+(2)$ state is

$$|Cr^+;B^6\Sigma^+(2)\rangle \approx 0.72|^6S;\ 3d^5\rangle + 0.60|^6D;\ 4s^13d^4\rangle$$

As the quality of the (valence) MRCI wave function improves from MRCI(+Q)/4Z to MRCI+DKH2(+Q)/4Z to MRCI(+Q)/5Z to MRCI+DKH2(+Q)/5Z, the binding energy becomes D_e = 85.0 (88.9), 83.7 (86.3), 83.4 (86.4), 84.6 (87.2) kcal/mol, respectively. On the other hand, at the highest CC level we get D_e[C-RCCSD(T)+DKH2/C5Z] = 86.9 kcal/mol. Note that while MRCI relativistic effects reduce (increase) the D_e by 1.3/4Z (1.2/5Z) kcal/mol, CC relativistic effects reduce the binding energy by more than 3 kcal/mol for both basis sets, 4Z and 5Z (Table 7). Disregarding the C-MRCI results on D_e due to large size nonextensivity effects, our "best" D_e value is 87 kcal/mol with respect to the adiabatic atoms. This compares favorably with the latest experimental value, $D_0^o = 90.0 \pm 1.3$ kcal/mol;[33b] the (indirect) theoretical value of Harrison and Hutchison is $D_e(=D_0 + \omega_e/2) = 84.3$ kcal/mol.[56]

Relativistic and core effects, strictly additive at the MRCI/5Z level and with the former more important than the latter, bring the bond distance to r_e(C-MRCI+DKH2+Q/C5Z) = 2.193 Å, in perfect agreement with the experimental number 2.1940 Å.[54] Similar results and trends are observed through the CC bond distance calculations, but at the highest level,C-RCCSD(T)+DKH2/C5Z, the r_e is underestimated by 0.02 Å as compared to experiment. It should be mentioned at this point, however, that we encountered severe convergence problems with the CC calculations of the X $^6\Sigma^+$ state.

Concerning now the dipole moment of the X-state, our results range wildly depending on the method and basis set. Based on the MRCI+DKH2/5Z, C-MRCI+DKH2/C5Z, and C-RCCSD(T)+DKH2/C5Z results, our recommended dipole moment calculated through the finite field method (μ_{FF}) is μ_e = 6.0 D, and certainly not larger than 6.5 D.

The next two states, A $^6\Pi(1)$ and B $^6\Sigma^+(2)$ which correlate adiabatically to (^5D; $4s^23d^4$) and (^5S; $4s^13d^5$) + Cl(^2P; M_L=0),

respectively, are very close in energy the experimental B $^6\Sigma^+(2)$−A $^6\Pi(1)$ splitting being close to 600 cm^{-1}.[53] We corroborate theoretically this practical degeneracy between these two states, but our calculations are uncertain as to their ordering (see below). According to ref 55 the A $^6\Pi(1)$ state is located 8870 cm^{-1} above the X-state. Depending on the method and basis set the range of our calculated T_e is ∼6000 (C-MRCI+DKH2/C4Z) to 9700 cm^{-1} [C-RCCSD(T)/C5Z]. The best agreement with the experimental T_e is obtained at the MRCI+Q/4Z, RCCSD(T)/4Z and RCCSD(T)/5Z levels, 8667, 8768, and 8810 cm^{-1}, respectively, due to cancelation effects; the MRCI+Q/5Z value of T_e = 7481 cm^{-1} can also be considered as acceptable. The ordering E[B $^6\Sigma^+(2)$]−E[A $^6\Pi(1)$] is +384 (−126) [MRCI(+Q)/4Z], −532 (−1442) [C-MRCI(+Q)/C4Z], +2729 (+2906) [MRCI(+Q)/5Z], +118 (−886) [MRCI+DKH2(+Q)/5Z] cm^{-1}. These wild fluctuations do not permit to draw any conclusions as to the ordering of these two states, but we are also allowed to express some doubts for the experimental B $^6\Sigma^+(2)$-A $^6\Pi(1)$ splitting of about +600 cm^{-1}.[53]

The μ_{FF} dipole moment of the A $^6\Pi(1)$ state is calculated to be 2.9 (MRCI) and 2.5 (CC) D, practically invariant to the level of each particular approach, MRCI or CC; the dipole moment of the B $^6\Sigma^+(2)$ state is μ_{FF} = 3.0 D. Notice that the finite field approach "normalizes" the μ_e value close to 3.0 D, whereas expectation values range from 3.1 to 5.2 D depending on the MRCI level and basis set.[27] Finally, the bond distance of A $^6\Pi(1)$ converges to r_e = 2.248 Å at the C-MRCI+DKH2+Q/C5Z level and to r_e = 2.239 [C-RCCSD(T)/C5Z] + [r_e(RCCSD(T) + DKH2/5Z)−r_e(RCCSD(T)/5Z] = 2.239−0.004 = 2.235 Å as contrasted to the experimental estimate of 2.23 Å.[55]

For the B $^6\Sigma^+(2)$ state our MRCI+Q/5Z r_e is 0.03 Å longer than the experimental one.[53] Distressingly enough, the addition of scalar relativistic effects increases the bond distance to 2.319 Å (MRCI+DKH2+Q/5Z) as contrasted to the experimental value of 2.270 Å.[53]

There is no much to be said for the four higher states, namely a $^4\Sigma^+(1)$, C $^6\Delta(1)$, b $^4\Pi(1)$, and c $^4\Delta(1)$. All our CrCl results from this point on are based at the MRCI(+Q)/4Z level of theory. The a $^4\Sigma^+(1)$ and C $^6\Delta(1)$ states are in essence degenerate, whereas the b $^4\Pi(1)$ and c $^4\Delta(1)$ are well separated, and therefore their ordering is certain. More or less similar results have been obtained for those four states by Harrison and Hutchison at the C-MRCI+CG+Q/ANO level[56] (Table 7). Figure 7 compares the calculated ordering of the first seven states between the isovalent species CrF[3] and CrCl at the same level of theory.

B. States $^4\Gamma(1)$, $^4\Sigma^-(1)$, $^4\Phi(1)$, $^4\Delta(2)$, $^4\Pi(2)$, $^4H(1)$, $^4\Pi(3)$, $^4\Sigma^+(2)$, $^4\Delta(3)$, $^4\Sigma^-(2)$, $^2\Gamma(1)$, $^2\Phi(1)$, $^2H(1)$, $^2\Delta(1)$, $^2\Pi(1)$, and $^2\Pi(2)$. A low-resolution energy ordering of the 16 states above, 10 quartets and 6 doublets all bound with respect to ground-state atoms Cr(^{7}S) + Cl(^{2}P), is shown in Figure 7; these are congested within an energy range of 0.73 eV. We recall that no experimental or theoretical data exist in this energy region; henceforth we limit ourselves to some general remarks.

(a) All states are strongly multireference and strongly ionic with an equilibrium charge transfer from Cr to Cl(^{2}P; M_L=0) of 0.6 to 0.65 electrons.

(b) All states are strongly bound with respect to adiabatic neutral atoms although we cannot be certain as to their correlation channels; the end products shown in Figure 6 are only indicative.

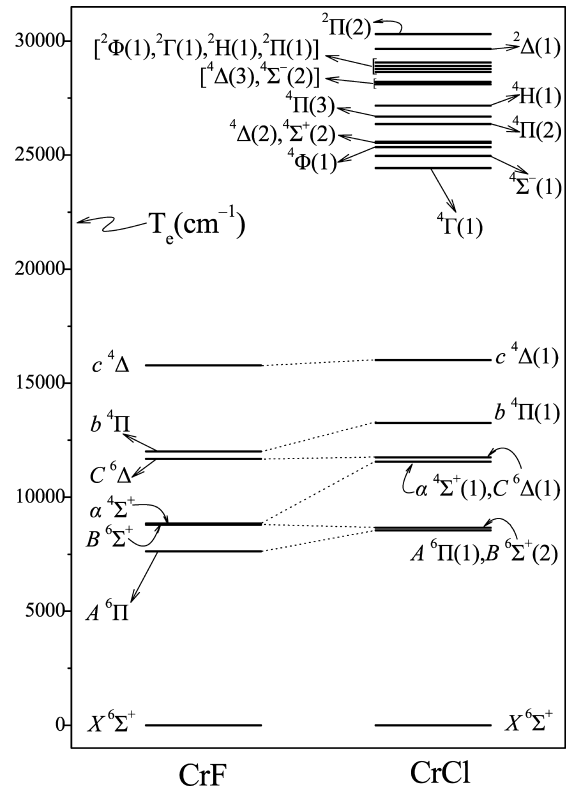

Figure 7. Comparative energy level diagram between calculated states of the isovalent species CrF and CrCl.

(c) The dipole moments obtained by the finite field method (μ_{FF}) range from 2.5 to 4.9 D. Notice again the large differences between $\langle\mu\rangle$ and μ_{FF}; on the average $\mu_{FF} - \langle\mu\rangle \approx$ 0.8 D.

(d) All 16 states have very similar bond distances centered around 2.20 Å; on the average r_e = 2.20 ± 0.02 Å.

8. Results and Discussion on the Charged Species

In what follows we discuss first the cations MCl^+ (section A) and then the anions MCl^- (section B), M = Sc−Cr.

A. ScCl$^+$, TiCl$^+$, VCl$^+$, and CrCl$^+$. No experimental or theoretical results are available on $ScCl^+$ and VCl^+. On $CrCl^+$ there is only one ab initio work by Alvarado-Swaisgood and Harrison; they report r_e, D_e, ω_e, and PECs for the X $^5\Sigma^+$ and A $^5\Pi$ states at the MCSCF+1+2/[5s4p3d/$_{Cr}$4s4p2d/$_{Cl}$] level.[58]

Since 1990 when the emission band system of $TiCl^+$ in the yellow-green region was recorded for the first time by Balfour and Chandrasekhar,[59] $TiCl^+$ has been the subject of a significant number of experimental studies. A condensed description of the literature on $TiCl^+$ is given in a recent paper by Halfen and Ziurys.[60] These workers analyzed the pure rotational spectrum of the X $^3\Phi$ state of $TiCl^+$, obtaining a bond distance r_0 = 2.188 79(7) Å by averaging the bond distances of the three isotopomers $^{48}Ti^{35}Cl^+$, $^{48}Ti^{37}Cl^+$, and $^{46}Ti^{35}Cl^+$. Finally the dissociation energy of $TiCl^+$ has been measured by Kneen et al.[61] through electron impact ionization study of $TiCl_n^+$ (n = 1−4) clusters; in particular $D(TiCl^+)$ = 102 kcal/mol.

For the cations $ScCl^+$, $TiCl^+$, VCl^+, and $CrCl^+$ we have studied the states (X $^2\Delta$, A $^2\Pi$, B $^2\Sigma^+$), (X $^3\Phi$, A $^3\Delta$, B $^3\Sigma^-$, C $^3\Pi$), (X $^4\Pi$, A $^4\Sigma^-$, B $^4\Delta$), and (X $^5\Sigma^+$, A $^5\Pi$, B $^5\Delta$), respectively, at the MRCI/5Z level and around equilibrium. The simplest way of thinking the formation of the MCl^+s is by removing one electron from the neutral species. With no exception the above MCl^+ states emerge by removing the $3\sigma^1$

TABLE 8: Total Energies E (E_h), Dissociation Energies D_e (kcal/mol), Bond Distances r_e (Å), Harmonic Frequencies ω_e (cm^{-1}), Mulliken Charges on M (q_M), and Energy Separations T_e (cm^{-1}) of $Sc^{35}Cl^+$, $^{48}Ti^{35}Cl^+$, $V^{35}Cl^+$, and $Cr^{35}Cl^+$at the MRCI(+Q)/5Z Level of Theory

species/state[a]	$-E$	D_e[b]	r_e	ω_e	q_M	T_e
$ScCl^+/X\ ^2\Delta$	1219.391590	102.4	2.275	467	+1.46	0.0
	(1219.41044)	(104.6)	(2.274)	(463)		(0.0)
$/A^2\Pi$	1219.378414	94.2	2.302	451	+1.50	2892
	(1219.39797)	(96.8)	(2.302)	(449)		(2737)
$/B^2\Sigma^+$	1219.376800	93.2	2.238	430	+1.48	3246
	(1219.39800)	(96.8)	(2.227)	(411)		(2732)
$TiCl^+/X\ ^3\Phi$	1308.050755	93.5	2.224	473	+1.39	0.0
	(1308.07337)	(97.3)	(2.219)	(474)		(0.0)
$/A^3\Delta$	1308.045074	90.0	2.199	447	+1.31	1247
	(1308.06935)	(94.8)	(2.186)	(439)		(881)
$/B^3\Sigma^-$	1308.044384	89.5	2.220	481	+1.32	1398
	(1308.06703)	(93.3)	(2.213)	(475)		(1391)
$/C^3\Pi$	1308.042821	88.5	2.230	446	+1.37	1741
	(1308.06578)	(92.5)	2.223	(441)		(1666)
expt ($^3\Phi$)		102[c]	2.18879(7)[d]	488.66[e]		
$VCl^+/X\ ^4\Pi$	1402.531142	86.7	2.171	477	+1.32	0.0
	(1402.55781)	(91.6)	(2.160)	(482)		(0.0)
$/A^4\Sigma^-$	1402.528774	85.2	2.159	432	+1.35	520
	(1402.55736)	(91.4)	(2.139)	(423)		(97)
$/B^4\Delta$	1402.527545	84.4	2.198	469	+1.34	789
	(1402.55239)	(88.2)	(2.191)	(464)		(1189)
$CrCl^+/X\ ^5\Sigma^+$	1502.977650	54.0	2.141	490	+1.30	0.0
	(1503.00688)	(52.6)	(2.132)	(493)		(0.0)
$/X^5\Sigma^{+f}$	1502.78949	47.3	2.19	475		0.0
$/A^5\Pi$	1502.967107	47.4	2.136	461	+1.34	2314
	(1502.99963)	(48.1)	(2.117)	(451)		(1589)
$/A^5\Pi^f$	1502.78082	41.9	2.17	481		1902
$/B^5\Delta$	1502.949672	36.4	2.176	435	+1.32	6140
	(1502.97832)	(34.7)	(2.165)	(471)		(6268)

[a] MRCI(+Q)/5Z adiabatic ionization energies of ScCl, TiCl, VCl, and CrCl are 6.35 (6.42), 6.69 (6.72), 7.04 (7.04), and 7.81 (7.93) eV, respectively. [b] D_e with respect to the ground state fragments M^++Cl(^{2}P; M_L=0). [c] Reference 41. [d] r_0 value; ref 60. [e] Reference 62. [f] Reference 58.

electron from the corresponding neutral states, namely, (a $^3\Delta$(1), b $^3\Pi$(1), c $^3\Sigma^+$(1)), (X $^4\Phi$, C $^4\Delta$, A $^4\Sigma^-$, B $^4\Pi$), (A $^5\Pi$, B $^5\Sigma^-$, X $^5\Delta$), and (X $^6\Sigma^+$, A $^6\Pi$, C $^6\Delta$) (vide supra). For instance, the leading MRCI CFs of the MCl^+ ground states are (using the convention previously introduced)

$$|X^2\Delta\rangle_{A_1} \approx 0.96|1\delta_+^1\rangle$$

$$|X^3\Phi\rangle_{B_1} \approx {}^1/_{\sqrt{2}}|2\pi_x^1 1\delta_+^1 + 2\pi_y^1 1\delta_-^1\rangle$$

$$|X^4\Pi\rangle_{B_1} \approx 0.75|2\pi_y^1 1\delta_+^1 1\delta_-^1\rangle + 0.41(|4\sigma^1 2\pi_x^1 1\delta_-^1\rangle + |4\sigma^1 2\pi_y^1 1\delta_+^1\rangle)$$

and

$$|X^5\Sigma^+\rangle_{A_1} \approx 0.94|2\pi_x^1 2\pi_y^1 1\delta_+^1 1\delta_-^1\rangle$$

for $ScCl^+$, $TiCl^+$, VCl^+, and $CrCl^+$, respectively.

Table 8 lists all our numerical results on these cations. Observe that, as in the corresponding MF^+s,[3] the MCl^+ cations are rather ionic with about 0.4 e^- transferred from M^+ to the Cl(^{2}P) atom. In addition, the ordering of the first MF^+ states is very similar to the MCl^+ species, i.e., (X $^2\Delta$, A $^2\Sigma^+$, B $^2\Pi$), (X $^3\Phi$, A $^3\Sigma^-$, B $^3\Pi$, C $^3\Delta$), (X $^4\Pi$, A $^4\Delta$, B$^4\Sigma^-$), (X $^5\Sigma^+$, A $^5\Pi$, C $^5\Delta$) for ScF^+, TiF^+, VF^+, and CrF^+, respectively.[3]

All of the calculated MCl^+ states, with the exception of A $^5\Pi$ and B $^5\Delta$ of $CrCl^+$, correlate to the ground state fragments M^++Cl(^{2}P; M_L=0). The end products of A $^5\Pi$ and B$^5\Delta$ states of $CrCl^+$ are Cr^+(^{6}D;M_L=±1,±2) + Cl(^{2}P; M_L=0). With respect to the ground-state atoms M^++Cl(^{2}P), the MRCI+Q /5Z binding energies of the X-MCl^+ states are quite large, monotonically decreasing from $ScCl^+$ to $CrCl^+$ (105, 97, 92, and 53 kcal/mol), and quite similar to the X-states of the corresponding neutrals with the exception of CrCl whose MRCI+Q /5Z D_e = 86 kcal/mol (vide supra).

Concerning the bond distances, and using our experience from the neutrals where the core ($3s^23p^6$) of M and scalar relativistic effects amount on the average to a bond shortening of 0.03 Å, our recommended r_e values of the X-$ScCl^+$, $TiCl^+$, VCl^+ and $CrCl^+$ states are 2.24, 2.19, 2.13, and 2.10 Å, respectively. It is encouraging that the experimental value of the X $^3\Phi$ state of $TiCl^+$ obtained by Halfen and Ziurys is r_0 = 2.188 79(7) Å,[60] as contrasted to 2.19 Å estimated presently.

For $CrCl^+$ it is fair to say that the MCSCF+1+2 results of Alvarado-Swaisgood and Harrison,[58] despite that our total energy is lower by one-third of a hartree, compare very favorably with ours; see Table 8.

Finally, from the T_e results on VCl^+, it is obvious that the X $^4\Pi$ and A $^4\Sigma^-$ states are degenerate at the MRCI+Q level, with the $^4\Pi$ state being formally the ground state.

B. $ScCl^-$, $TiCl^-$, VCl^-, and $CrCl^-$. As was mentioned in the Introduction, there is a complete lack of either experimental or theoretical results on the MCl^- anions. In the field of the spherical anion Cl^-(^{1}S) the ground states of Sc(^{2}D), Ti(^{3}F), V(^{4}F), and Cr(^{7}S) give rise to the low-lying Λ−Σ MCl^- states ($^2\Sigma^+$, $^2\Pi$, $^2\Delta$), ($^3\Sigma^-$, $^3\Pi$, $^3\Delta$, $^3\Phi$), ($^4\Sigma^-$, $^4\Pi$, $^4\Delta$, $^4\Phi$), and $^7\Sigma^+$, respectively. Using the RCCSD(T)/5Z method, we have constructed PECs for the first three states of $ScCl^-$ (X $^2\Delta$, A $^2\Pi$, B $^2\Sigma^+$), for three out of four states of $TiCl^-$ (X $^3\Phi$, $^3\Sigma^-$,$^3\Delta$), two out of four states of VCl^- (X $^4\Delta$, $^4\Pi$) and the X $^7\Sigma^+$ of $CrCl^-$. These RCCSD(T)/5Z curves are displayed

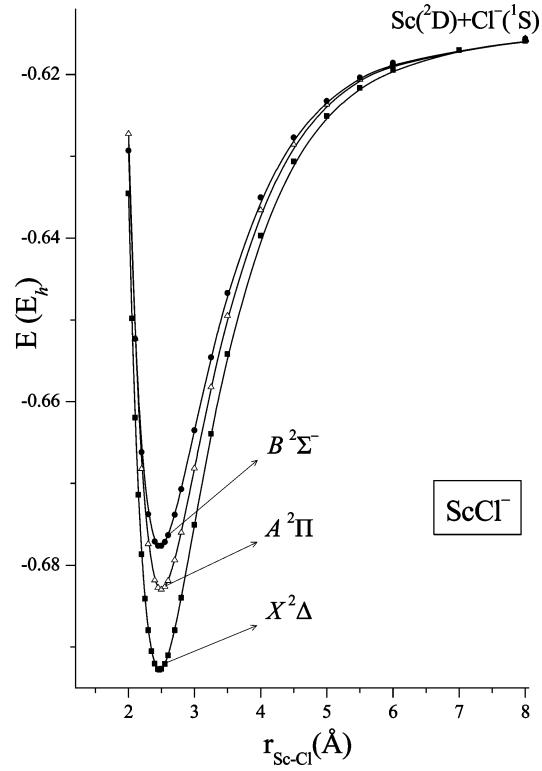

Figure 8. RCCSD(T)/5Z potential energy curves of the $ScCl^-$ anion. Energies are shifted by +1219 E_h.

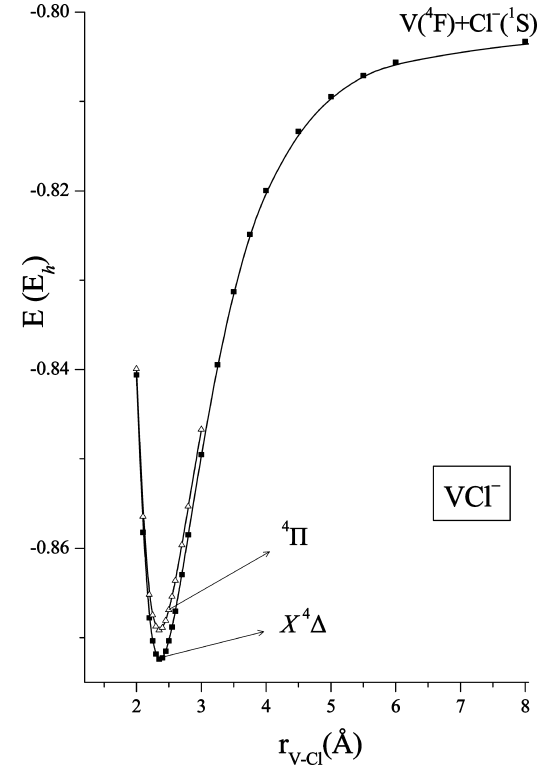

Figure 10. RCCSD(T)/5Z potential energy curves of the VCl^- anion. Energies are shifted by +1402 E_h.

in Figures 8, 9, 10, and 11 whereas our numerical findings are listed in Table 9.

Our general observations on the MCl^- anions are the following. All examined states are relatively strongly bound with D_e values decreasing monotonically from $ScCl^-$ (49.3 kcal/mol) to $CrCl^-$(33.6 kcal/mol). The bonding is caused by a flow of about 0.6 e^- from Cl^- to Sc, Ti, and V, and 0.3 e^- to Cr (populations at the Hartree−Fock level). The same, but with a smaller charge migration (0.4−0.2 e^-) from F^- to M, was

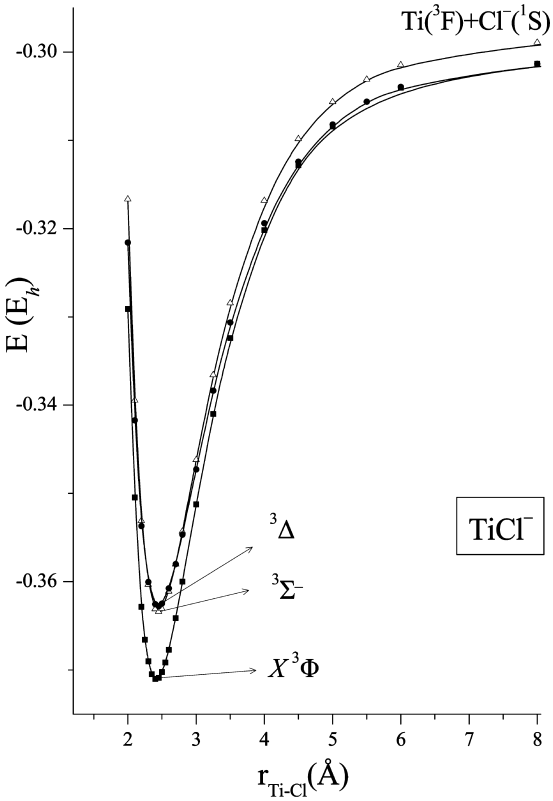

Figure 9. RCCSD(T)/5Z potential energy curves of the $TiCl^-$ anion. Energies are shifted by +1308 E_h.

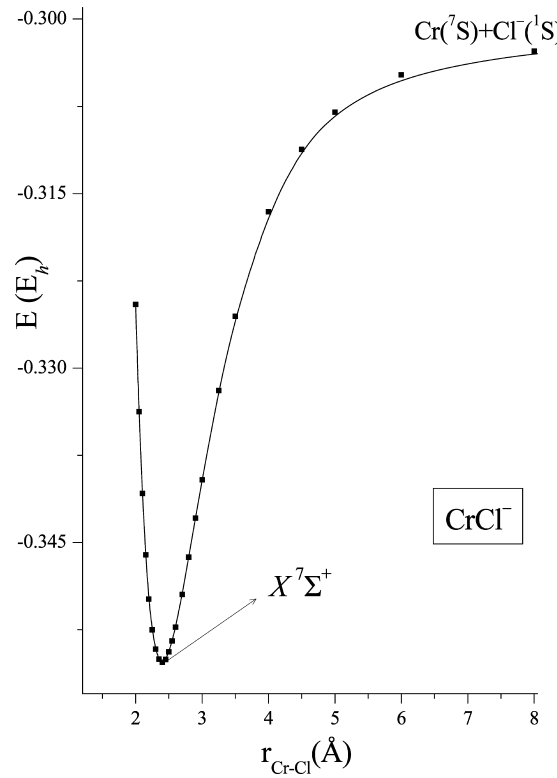

Figure 11. RCCSD(T)/5Z potential energy curves of the $CrCl^-$ anion. Energies are shifted by +1503 E_h.

TABLE 9: Total Energies E (E_h), Dissociation Energies D_e (kcal/mol), Bond Distances r_e (Å), Harmonic Frequencies ω_e (cm^{-1}), Mulliken Charges on M (q_M), and Energy Separations T_e (cm^{-1}) of $Sc^{35}Cl^-$, $^{48}Ti^{35}Cl^-$, $V^{35}Cl^-$, and $Cr^{35}Cl^-$ at the RCCSD(T)/5Z Level of Theory

species/state[a]	$-E$	D_e[b]	r_e	ω_e	q_M[c]	T_e
$ScCl^-/X\ ^2\Delta$	1219.692758	49.3	2.472	309	−0.59	0.0
$/A^2\Pi$	1219.682983	43.1	2.494	291	−0.58	2145
$/B^2\Sigma^+$	1219.677684	40.0	2.473	277	−0.56	3308
$TiCl^-/X\ ^3\Phi$	1308.371044	44.5	2.415	306	−0.65	0.0
$/^3\Sigma^-$	1308.363395	40.1	2.447	293	−0.52	1679
$/^3\Delta$	1308.362766	39.7	2.445	276	−0.60	1819
$VCl^-/X\ ^4\Delta$	1402.872449	43.5	2.363	311	−0.67	0.0
$/^4\Pi$	1402.869174	41.4	2.354	306	−0.69	719
$CrCl^-/X\ ^7\Sigma^+$	1503.355300	33.6	2.398	266	−0.30	0.0

[a] The RCCSD(T)/5Z EAs of ScCl, TiCl, VCl, and CrCl are 1.21, 1.27, 1.23, and 1.15 eV, respectively. [b] With respect to the ground state fragments $M+Cl^-(^1S)$. [c] Hartree−Fock Mulliken charges.

TABLE 10: Dissociation Energies D_e (kcal/mol), Bond Distances r_e (Å), and Dipole Moments μ_e for the MCl and $MCl^\pm$ Species, M = Sc, Ti, V, and Cr. Experimental Results in Parentheses

species	X-state	D_e	r_e	μ_e
ScCl	$^1\Sigma^+$	107 ± 1	2.227	2.5
	$(^1\Sigma^+)$	(∼120)	(2.2303)	
TiCl	$^4\Phi$	99	2.273	3.8
	$(^4\Phi)$	(101.9 ± 2)	(2.2646)	
VCl	$^5\Delta$ ($^5\Pi$?)	98	2.230	4.3
	$(^5\Delta)$	(102.5 ± 2)	(2.2145)	
CrCl	$^6\Sigma^+$	87	2.193	6.0
	$(^6\Sigma^+)$	(90.6 ± 1.3)	(2.1939)	
$ScCl^+$	$^2\Delta$	105	2.24	
$TiCl^+$	$^3\Phi$	97	2.19	
	$(^3\Phi)$	(102)	(2.1888, r_0)	
VCl^+	$^4\Pi$ ($^4\Sigma^-$?)	92	2.13	
$CrCl^+$	$^5\Sigma^+$	53	2.10	
$ScCl^-$	$^2\Delta$	49	2.472	
$TiCl^-$	$^3\Phi$	45	2.415	
VCl^-	$^4\Delta$	44	2.363	
$CrCl^-$	$^7\Sigma^+$	34	2.398	

observed in the corresponding fluorides MF^-, where we refer for a more extended discussion on the bonding.[5] For the $X\ ^4\Delta$ and $^4\Pi$ states of VCl^- the same Mulliken atomic distributions were also obtained at the MRCI/5Z level, so the HF charges seem quite reliable. Contrasting the binding energies of the ground-state MF^-s (the same as in MCl^-s) to the X-states of the MCl^-s, the former are larger than the latter by a factor of about 1.7, that is, $D_e(MF^-) \approx 1.7 \times D_e(MCl^-)$, while $r_e(MF^-) \approx 0.83 \times r_e(MCl^-)$.

9. Summary

The present work is a comprehensive ab initio study of the neutral diatomic chlorides MCl and their ions $MCl^\pm$ (M = Sc, Ti, V, Cr), by MRCI and RCCSD(T) methods and large correlation consistent basis sets. We have studied a total of 71, 13, and 9 states for the MCl, MCl^+, and MCl^-, respectively, and we have constructed full potential energy curves for all MCl and MCl^- states. Most of our results are reported for the first time; in particular, concerning the cations, only one ab initio work on $CrCl^+$ was published 20 years ago,[58] whereas the MCl^- species have never been studied before either experimentally or theoretically. Overall, our findings are in good agreement with available experimental numbers.

Table 10 recapitulates D_e, r_e, and μ_e (MCl) of the ground states of all species studied in the present work; for easy comparison available experimental results are also included. It can be seen that the agreement with experiment is fairly good considering the inherent difficulties of these diatomics.

Both the neutral and cationic MCl species are quite ionic with a charge transfer of more than 0.6 e^- from M to Cl and about 0.4 e^- from M^+ to Cl. Finally, the similarity with the corresponding fluorides, MF and $MF^\pm$ is rather remarkable: the ground states are of the same symmetry whereas the same trends are followed in D_e, r_e, and even μ_e values.

We believe that this comprehensive ab initio work on the MCl and $MCl^\pm$ species can be proved useful to the people working with the same or analogous molecular systems.

References and Notes

(1) See for instance: Stanton, J. F.; Gauss, T. *Advances in Chemical Physics*; Prigogine, I., Rice, S. A., Eds.; Wiley: New York, 2003; p 101, and references therein.

(2) Harrison, J. F. *Chem. Rev.* **2000**, *100*, 679.

(3) Koukounas, C.; Kardahakis, S.; Mavridis, A. *J. Chem. Phys.* **2004**, *120*, 11500.

(4) Koukounas, C.; Mavridis, A. *J. Phys. Chem. A* **2008**, *112*, 11235–11250.

(5) Kardahakis, S.; Koukounas, C.; Mavridis, A. *J. Chem. Phys.* **2005**, *122*, 054312.

(6) (a) Balabanov, N.; Peterson, K. A. *J. Chem. Phys.* **2005**, *123*, 064107. (b) Balabanov, N.; Peterson, K. A. *J. Chem. Phys.* **2006**, *125*, 074110.

(7) (a) Dunning, T. H., Jr. *J. Chem. Phys.* **1989**, *90*, 1007; Woon, D. E.; Dunning, T. H., Jr. *J. Chem. Phys.* **1993**, *98*, 1358. (b) Peterson, K. A.; Dunning, T. H., Jr. *J. Chem. Phys.* **2002**, *117*, 10548.

(8) Douglas, M.; Kroll, N. M. *Ann. Phys. (N.Y.)* **1974**, *82*, 89.

(9) Hess, B. A. *Phys. Rev. A: At. Mol. Opt. Phys.* **1985**, *32*, 756. Hess, B. A. *Phys. Rev. A: At. Mol. Opt. Phys.* **1986**, *33*, 3742.

(10) de Jong, W. A.; Harrison, R. J.; Dixon, D. A. *J. Chem. Phys.* **2001**, *114*, 48.

(11) Raghavachari, K.; Trucks, G. W.; Pople, J. A.; Head-Gordon, M. *Chem. Phys. Lett.* **1989**, *157*, 479. Watts, J. D.; Bartlett, R. J. *J. Chem. Phys.* **1993**, *98*, 8718. Knowles, P. J.; Hampel, C.; Werner, H.-J. *J. Chem. Phys.* **1993**, *9*, 5219. Knowles, P. J.; Hampel, C.; Werner, H.-J. *J. Chem. Phys.* **2000**, *112*, 3106E.

(12) Werner, H.-J.; Knowles, P. J. *J. Chem. Phys.* **1988**, *89*, 5803. Knowles, P. J.; Werner, H.-J. *Chem. Phys. Lett.* **1988**, *145*, 514.

(13) Jansen, H. B.; Ross, P. *Chem. Phys. Lett.* **1969**, *3*, 140. Boys, S. F.; Bernardi, F. *Mol. Phys.* **1970**, *19*, 553.

(14) MOLPRO 2000 is a package of ab initio programs designed by H.-J. Werner and P. J. Knowles, version 2002.6; (a) Amos, R. D.; Bernhardsson, A.; Berning, A.; Celani, P.; Cooper, D. L.; Deegan, M. J. O.; Dobbyn, A. J.; Eckert, F.; Hampel, C.; Hetzer, G.; Knowles, P. J.; Korona, T.; Lindh, R.; Lloyd, A. M.; McNicholas, S. J.; Manby, F. R.; Meyer, W.; Mura, M. E.; Nicklass, A.; Palmieri, P.; Pitzer, R.; Rauhut, G.; Schütz, M.; Schumann, U.; Stoll, H.; Stone, A. J.; Tarroni, R.; Thorsteinsson, T.; Werner, H.-J.

(15) ACESII is a program product of Quantum Theory Project, University of Florida; J. F. Stanton, J. Gauss, J. D. Watts, et al. Integral packages included are VMOL (J. Almlöf and P. R. Taylor); VPROPS (P. R. Taylor); and ABACUS (T. Helgaker, H. J. Aa. Jensen, P. Jørgensen, J. Olsen, and P. R. Taylor).

(16) Ralchenko, Yu.; Kramida, A. E.; Reader, J. and NIST ASD Team (2008). NIST Atomic Spectra Database (version 3.1.5), [Online]. Available: http://physics.nist.gov/asd3 [2009, January 31]. National Institute of Standards and Technology, Gaithersburg, MD.

(17) Berzinsh, U.; Gustafsson, M.; Hanstorp, D.; Klinkmüller, A.; Ljungblad, U.; Mårtensson-Pendrill, A. M. *Phys. Rev. A* **1995**, *51*, 231.

(18) Taher, F.; Effantin, C.; Bernard, A.; d'Incan, J.; Vergès, J.; Shenyavskaya, E. A. *J. Mol. Spectrosc.* **1997**, *184*, 880, and references therein.

(19) Taher, F.; Effantin, C.; Bernard, A.; d'Incan, J.; Shenyavskaya, E. A.; Vergès, J. *J. Mol. Spectrosc.* **1996**, *179*, 223.

(20) Adam, A. G.; Peers, J. R. D. *J. Mol. Spectrosc.* **1997**, *182*, 215.

(21) Lin, W.; Beaton, S. A.; Evans, C. J.; Gerry, M. C. L. *J. Mol. Spectrosc.* **2000**, *199*, 275.

(22) Huber, K. P.; Herzberg, G. *Molecular Spectra and Molecular Structure: IV Constants of Diatomic Molecules*; Van Nostrand, Reinhold: New York, 1979,

(23) de Blasi Bourdon, E. B.; Prince, R. H. *Surf. Sci.* **1984**, *144*, 581.

(24) Langhoff, S. R.; Bauschlicher, C. W., Jr.; Partridge, H. *J. Chem. Phys.* **1988**, *89*, 396.

(25) Boutassetta, N.; Allouche, A. R.; Aubert-Frécon, M. *J. Phys. B: At. Mol. Opt. Phys.* **1996**, *29*, 1637.

(26) Taher-Mansour, F.; Allouche, A.; Korek, M. J. *J. Mol. Spectrosc.* **2008**, *248*, 6125.
(27) Tzeli, D.; Mavridis, A. *J. Chem. Phys.* **2003**, *118*, 4984. *Ibid.* **2005**, *122*, 056101.
(28) Shenyavskaya, E. A.; Lebeault-Dorget, M.-A.; Effantin, C.; d'Incan, J.; Bernard, A.; Vergès, J. *J. Mol. Spectrosc.* **1995**, *171*, 309.
(29) Effantin, C.; Shenyavskaya, E. A.; d'Incan, J.; Bernard, A.; Topouzkhanian, A.; Wannous, G. *J. Mol. Spectrosc.* **1997**, *185*, 249.
(30) Kaledin, L. A.; McCord, J. E.; Heaven, M. C. *J. Mol. Spectrosc.* **1995**, *171*, 569.
(31) Lebeault-Dorget, M.-A.; Effantin, C.; d'Incan, J.; Bernard, A.; Shenyavskaya, E. A.; Vergès, J. *J. Chem. Phys.* **1995**, *102*, 708.
(32) Shenyavskaya, E. A.; Ross, A. J.; Topouzkhanian, A.; Wannous, G. *J. Mol. Spectrosc.* **1993**, *162*, 327.
(33) (a) Hildenbrand, D. L. *J. Phys. Chem. A* **2009**, *113*, 1472. (b) *ibid.* **2008**, *112*, 3813.
(34) Ram, R. S.; Bernath, P. F. *J. Mol. Spectrosc.* **1997**, *186*, 113.
(35) Maeda, A.; Hirao, T.; Bernath, P. F.; Amano, T. *J. Mol. Spectrosc.* **2001**, *210*, 250, and references therein.
(36) Adam, A. G.; Hopkins, W. S.; Sha, W.; Tokaryk, D. W. *J. Mol. Spectrosc.* **2006**, *236*, 42.
(37) Ram, R. S.; Bernath, P. F. *J. Mol. Spectrosc.* **1999**, *195*, 299.
(38) Boldyrev, A. I.; Simons, J. *J. Mol. Spectrosc.* **1998**, *188*, 138.
(39) Bauschlicher, C. W. *Theor. Chem. Acc.* **1999**, *103*, 141.
(40) Sakai, Y.; Mogi, K.; Miyoshi, E. *J. Chem. Phys.* **1999**, *111*, 3989.
(41) Focsa, C.; Bencheikh, M.; Pettersson, G. M. *J. Phys. B: At. Mol. Opt. Phys.* **1998**, *31*, 2857.
(42) Ram, R. S.; Bernath, P. F. *J. Mol. Spectrosc.* **2004**, *227*, 43.
(43) Imajo, T.; Wang, D. B.; Tanaka, K.; Tanaka, T. *J. Mol. Spectrosc.* **2000**, *203*, 216.
(44) Iacocca, D.; Chatalic, A.; Deshamps, P.; Pannetier, G. *Compt. Rend. C* **1970**, *271*, 669.
(45) Ram, R. S.; Bernath, P. F.; Davis, S. P. *J. Chem. Phys.* **2001**, *114*, 4457.
(46) Ram, R. S.; Liévin, J.; Bernath, P. F.; Davis, S. P. *J. Mol. Spectrosc.* **2003**, *217*, 186.
(47) Hildenbrand, D. L.; Lau, K. H.; Perez-Mariano, J.; Sanjurjo, A. *J. Phys. Chem. A* **2008**, *112*, 9978.
(48) Dolg, M.; Wedig, C. I.; Stoll, H.; Preuss, H. *J. Chem. Phys.* **1987**, *86*, 866. Bergner, A.; Dolg, M.; Kuechle, W.; Stoll, H.; Preuss, H. *Mol. Phys.* **1993**, *80*, 1431.
(49) Rao, V. R.; Rao, K. R. *Indian J. Phys.* **1949**, *23*, 508.
(50) Bulewicz, E. M.; Phillips, L. F.; Sugden, T. M. *Trans. Faraday Soc.* **1961**, *57*, 921.
(51) Milushin, M. I.; Gorokhov, L. N. *Russ. J. Phys. Chem.* **1988**, *62*, 387, as cited by Hildenbrand, D. L. *J. Chem. Phys.* **1995**, *103*, 2634.
(52) Oike, T.; Okabayashi, T.; Taminoto, M. *Astrophys. J.* **1995**, *445*, L67.
(53) Bencheikh, M.; Koivisto, R.; Launila, O.; Flament, J. P. *J. Chem. Phys.* **1997**, *106*, 6231.
(54) Oike, T.; Okabayashi, T.; Tanimoto, M. *J. Chem. Phys.* **1998**, *109*, 3501.
(55) Koivisto, R.; Launila, O.; Schimmelpfennig, B.; Simard, B.; Wahlgren, U. *J. Chem. Phys.* **2001**, *114*, 8855.
(56) Harrison, J. F.; Hutchison, J. H. *Mol. Phys.* **1999**, *97*, 1009.
(57) Nielsen, I. M. B.; Allendorf, M. D. *J. Phys. Chem. A* **2005**, *109*, 928.
(58) Alvarado-Swaisgood, A. E.; Harrison, J. F. *J. Phys. Chem.* **1988**, *92*, 5896.
(59) Balfour, W. J.; Chandrasekhar, K. S. *J. Mol. Spectrosc.* **1990**, *139*, 245.
(60) Halfen, D. T.; Ziurys, L. M. *J. Mol. Spectrosc.* **2005**, *234*, 34, and references therein.
(61) Kneen, K. R.; Leroi, G. E.; Allison, J. *Int. J. Mass Spectrom.* **1999**, *182/183*, 163.
(62) Focsa, C.; Pinchemel, B.; Féménias, J.-L.; Huet, T. R. *J. Chem. Phys.* **1997**, *107*, 10365.

JP901225Y